

# BENCHMARKING AND ENHANCING VLM FOR COMPRESSED IMAGE UNDERSTANDING

Zifu Zhang<sup>1,2\*</sup>, Tongda Xu<sup>1,3\*</sup>, Siqi Li<sup>1,4</sup>, Shengxi Li<sup>2†</sup>, Yue Zhang<sup>2</sup>, Mai Xu<sup>2</sup>, Yan Wang<sup>1†</sup>

<sup>1</sup>Institute for AI Industry Research, Tsinghua University

<sup>2</sup>Beihang University

<sup>3</sup>Department of Computer Science and Technology, Tsinghua

<sup>4</sup>Beijing University of Technology

LiShengxi@buaa.edu.cn, wangyan@air.tsinghua.edu.cn

## ABSTRACT

With the rapid development of Vision-Language Models (VLMs) and the growing demand for their applications, efficient compression of the image inputs has become increasingly important. Existing VLMs predominantly digest and understand high-bitrate compressed images, while their ability to interpret low-bitrate compressed images has yet to be explored by far. In this paper, we introduce the first comprehensive benchmark to evaluate the ability of VLM against compressed images, varying existing widely used image codecs and diverse set of tasks, encompassing over one million compressed images in our benchmark. Next, we analyse the source of performance gap, by categorising the gap from a) the information loss during compression and b) generalisation failure of VLM. We visualize these gaps with concrete examples and identify that for compressed images, only the generalization gap can be mitigated. Finally, we propose a universal VLM adaptor to enhance model performance on images compressed by existing codecs. Consequently, we demonstrate that a single adaptor can improve VLM performance across images with varying codecs and bitrates by 10%-30%. We believe that our benchmark and enhancement method provide valuable insights and contribute toward bridging the gap between VLMs and compressed images.

## 1 INTRODUCTION

The boom of multimedia services and applications has resulted in dramatic increase in image data, creating significant challenges in terms of transmission bandwidth and storage capacity. To address this, efficient image compression methods are essential for reducing data volume while maintaining or enhancing the subjective visual quality for human perception. Over the past few decades, numerous advanced compression standards have been introduced, such as JPEG (Wallace, 1991), and VTM (Bross et al., 2021), alongside recent end-to-end learned compression approaches (Ballé et al., 2018; Lu et al., 2019; Cheng et al., 2020; Zhang et al., 2025b) and generative compression methods (Mentzer et al., 2020; Li et al., 2024c; Zhang et al., 2025a).

In parallel, the advent of Big Data has transformed the way intelligent machines interact with the world, leading to extensive research into compression techniques for machine vision tasks, as opposed to human vision. Notable examples include image coding for machines (ICM) (Kang et al., 2022) and feature coding for machines (FCM) (Rosewarne, 2023), emerging

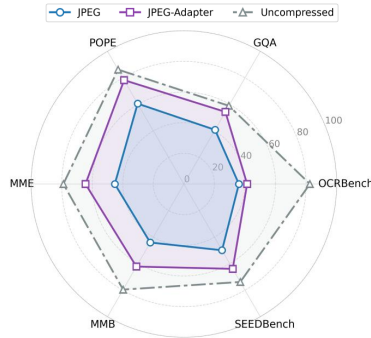


Figure 1: Visualization of VLM performance drop due to image compression and improvement by our method, measured by BD-Metric.

\*These authors contributed equally to this work.

†To whom correspondence should be addressed.

Questions	Uncompressed	Traditional Compression	Learning Compression	Generative Compression
Q1 What is written in the image?				
Q2 Are the curtains on the right or on the left?				
Q3 Which kind of furniture is green?				

Figure 2: Comparative visualization of four image compression technique: uncompressed, traditional codec (JPEG), learning-based codec (ELIC), and generative codec (StableCodec), highlighting their impact on visual clarity and semantic preservation through targeted question-answering. All forms of compression-induced distortion affect the ability of VLMs to understand images.

standards introduced by the moving picture experts group (MPEG). However, previous works (Kim et al., 2023; Zhang et al., 2024b; Chen et al., 2023a) have largely focused on specific computer vision tasks, such as object detection and instance segmentation, using fixed backbone networks, which limits their generalization capabilities.

With the continuous advancements in the multimodal field, VLMs have developed rapidly (Wang et al., 2024; Chen et al., 2025; 2024). Current VLMs are not only capable of understanding complex images (Yao et al., 2024) but also performing tasks such as object detection and segmentation (Feng et al., 2025), further generalizing and unifying visual tasks. This makes VLMs a promising and important direction for future development. To enhance the ability of VLMs to process compressed images, one approach is to optimize existing codecs to minimize the bitrate without compromising VLM performance. Research based on VCM and FCM has demonstrated good results when transferring tasks to VLM vision (Kao et al., 2024; Li et al., 2024a). However, these methods are specific to a particular codec or VLM, limiting the generalization capabilities. On the other hand, another approach is to improve the VLM’s capacity to understand compressed images from various codecs, independent of specific compression distortions. This approach could enhance generalization, but to date, no research has investigated this area. Furthermore, although several benchmarks exist to evaluate VLMs’ performance in tasks such as VQA (Hudson & Manning, 2019), spatial relations (Li et al., 2023a; Liu et al., 2024a; Li et al., 2023b), text understanding (Liu et al., 2024b), and knowledge answering (Yue et al., 2024), no benchmark has been developed specifically for assessing VLM performance on compressed images.

In this paper, we present a comprehensive benchmark designed to evaluate the ability of VLMs to understand and process compressed images. Our benchmark includes 11 widely-used codecs and 3 series of VLMs, ranging from 1 to 32 billion parameters, and assesses both coarse-grained and fine-grained metrics across more than 1 million compressed images. This large-scale analysis allows us to quantify the performance degradation of VLMs due to image compression, revealing that compression can significantly impair the model’s ability to interpret visual content, as reflected in the objective results shown in Figure 1 and the subjective examples in Figure 2. Based on this, we further break down the observed performance gap into two distinct components: the information gap during compression, which directly impacts the fidelity of image features, and the generalization gap of VLMs, which limits their ability to adapt to compressed images. Through visualizations and examples, we show that while the loss of information during compression is inherent and cannot be easily mitigated, the generalization gap represents a gap that can be addressed by improving the model’s ability to handle compressed inputs. To close this generalization gap, we propose a lightweight VLM adaptor that enhances VLM performance on compressed images across various codecs and bitrates. Empirical results show a 10%-30% improvement in understanding images compressed with different codecs, making it a promising solution for real-world applications involving image compression.

To wrap up, our contribution can be summarized as follows:

- We establish a comprehensive benchmark to explore the impact of image compression on VLM understanding, including more than 10 codecs and 1 million compressed images.
- We analyse the performance gap between compressed and uncompressed images, and propose the information and generalization gap, illustrated using JPEG and Qwen-VL2.5-3B.
- To eliminate generalization gap, we introduce a universal lightweight VLM adaptor to enhance performance on heavily compressed images across different codecs. Empirically, our adaptor improve by 10%-30%.

## 2 BENCHMARKING VLM FOR COMPRESSED IMAGES UNDERSTANDING

### 2.1 OVERVIEW

**Image Codecs.** We selected 11 state-of-the-art codecs with three representative categories, including traditional codecs, learning-based codecs, and generative codecs, as shown in Table 1. Specifically, for traditional codecs, we chose the widely used JPEG (Wallace, 1991), HM (Sullivan et al., 2012) and VTM (Bross et al., 2021). For learning-based codecs, we selected commonly used ELIC (He et al., 2022), TCM (Liu et al., 2023a), and MLICpp (Jiang et al., 2023). For generative codecs, we selected the GAN-based HiFiC (Mentzer et al., 2020) and MS-ILLM (ILLM) (Muckley et al., 2023), as well as the diffusion-based DiffEIC (D.EIC)(Li et al., 2024c), RDEIC (Li et al., 2025), and StableCodec (S.Codec) (Zhang et al., 2025a). All compression methods were applied to the original dataset with four different bitrate levels to cover a wide range of bitrates. Detailed parameter settings are provided in the Appendix A.

**Datasets and Tasks.** To assess the impact of image compression on VLMs, we curate seven tasks covering coarse-grained and fine-grained evaluation. Coarse-grained tasks focus on semantic understanding, evaluated using the POPE (Li et al., 2023b), GQA (Hudson & Manning, 2019) and COCO-Caption (COCOC) (Chen et al., 2015) benchmarks, which encompass common vision-language tasks such as visual question answering, spatial reasoning, and image captioning. For fine-grained tasks, we use OCRBench (OCRB) (Liu et al., 2024b), comprising 1000 images across various resolutions, allowing us to test codec adaptability to different image sizes. Additionally, we include three comprehensive benchmarks: MMBench (MMB) (Liu et al., 2024a), MME (Chaoyou et al., 2023), and SEEDBench (SEEDB) (Li et al., 2023a), to evaluate VLMs’ performance in perception, semantic understanding, and spatial reasoning with compressed images. All the results are evaluated by VLMEvalKit (Duan et al., 2024) and detailed descriptions of each task and their corresponding evaluation metrics are provided in Appendix B.

**Vision-Language Models.** Since different VLMs exhibit varying task performance, we evaluate several widely used open-source models, including Qwen-Chat-7B (Bai et al., 2023), Qwen-VL2.5-3B, Qwen-VL2.5-7B, Qwen-VL2.5-32B (Bai et al., 2025), Janus-pro-1B, Janus-pro-7B (Chen et al., 2025), InternVL3-1B, InternVL3-2B, and InternVL3-8B (Zhu et al., 2025), to compare VLMs with different parameter sizes. To quantify the impact of compression, we treat the results on uncompressed images in Appendix Figure 10 as the performance ceiling and measure degradation under different compression settings.

Table 1: Assessing 9 VLMs of varying scales and 11 representative image codecs with 7 metrics.

	Codecs (11)	Tasks (7)		VLMs (9)	
Traditional	JPEG, HM, VTM	Coarse-grained	POPE, GQA COCO-Caption	1-2B 3B	InternVL3, Janus-Pro Qwen2.5-VL
Learning-based	ELIC, TCM, MLICpp	Fine-grained	OCRBench	7-8 B	Qwen-Chat, Qwen2.5-VL Janus-Pro, InternVL3
Generative	HiFiC, MS-ILLM, DiffEIC, RDEIC, S.Codec	Comprehensive	MMB, MME, SEEDBench	32B	Qwen2.5-VL

## 2.2 CAN VLM UNDERSTAND COMPRESSED IMAGES

To evaluate whether VLMs can understand heavily images, we follow the setup outlined in Section 2.1 and find that a significant performance gap persists between uncompressed and compressed images for VLM vision. We state our main observations as follows:

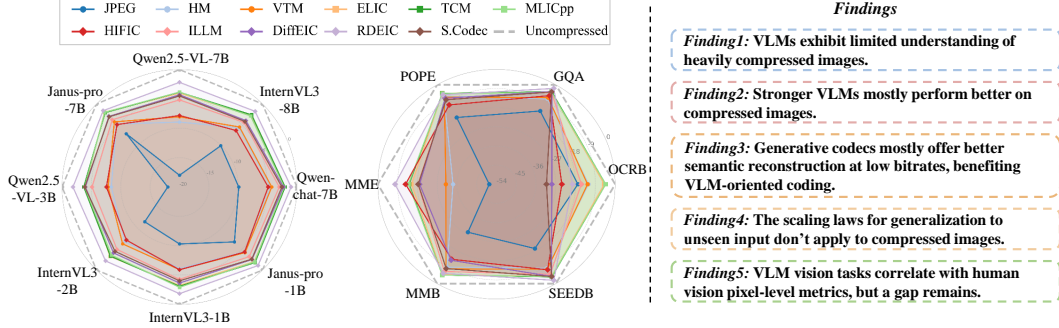


Figure 3: (a) BD-Metric values of different VLMs across different compression methods for the same tasks (SEEDBench). (b) BD-Metric values for different tasks under various compression methods based on the same VLM (Qwen-VL2.5-3B). (c) Summary of our main findings.

**Finding1: VLMs exhibit limited understanding of heavily compressed images.** Our evaluation indicates that VLMs face significant challenges when dealing with heavily compressed images, as evidenced in Figure 3. All radar plots of the compression methods fall within the boundary of the uncompressed baseline, showing varying degrees of performance degradation. Additionally, we plot the rate-metric curves for all tasks in Figure 4 based on Qwen-VL2.5-3B, and present the rate-metric curves for all other VLMs in Appendix C.1. When the bitrate falls below 0.1 bpp, VLMs struggle to maintain accurate semantic understanding and task performance, as compression artifacts distort crucial visual details. This finding suggests that VLMs' ability to process and comprehend images deteriorates as compression rates increase, particularly under high compression levels.

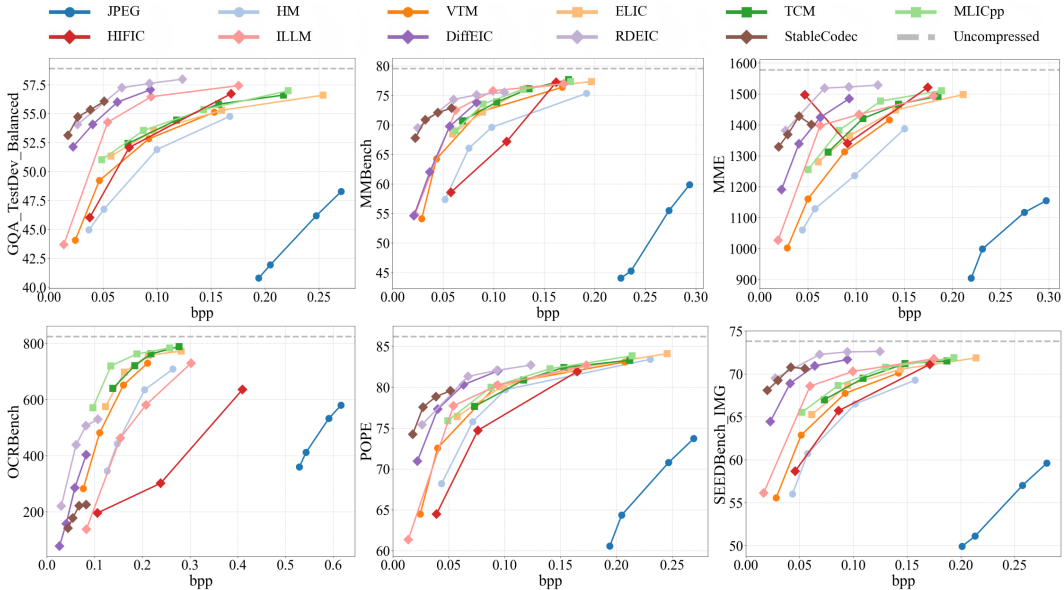


Figure 4: Rate-Metric curves for all types of codecs on six tasks using Qwen-VL2.5-3B. Specifically, the GQA metric is computed from five categories of questions. MMBench represents the weighted average of six evaluation dimensions, while MME denotes the aggregate of perception-related measures. OCRBench, POPE, and SEEDBench are weighted averages across five scene types, three sampling strategies, and nine spatial dimensions, respectively.

**Finding2: Stronger VLMs mostly perform better on compressed images.** By comparing the rate-distortion curves across different VLMs and the radar results presented in Figure 10 and Figure 20 in the Appendix, we observe that their relative performance rankings remain consistent with those under the uncompressed condition. This suggests that models with better performance on uncompressed images also demonstrate greater robustness to compressed images. However, as shown in Figure 3-(a), under the same task conditions, Janus-pro exhibits the smallest decrease in performance across all compression conditions, indicating that it has the best resistance to compression. This resilience is independent of the model’s absolute performance.

**Finding3: Generative codecs mostly offer better semantic reconstruction at low bitrates, benefiting VLM-oriented coding.** Compared to traditional and learning-based codecs, generative codecs, particularly those based on diffusion models, are more effective at preserving the semantic content of images. Codecs such as RDEIC and StableCodec excel in reconstructing semantically consistent images at lower bitrates, placing their curves in the upper-left corner of Figure 4, making them more suitable for tasks involving VLMs. In Table 2, we comprehensively evaluate different codecs based on various VLMs and tasks using the ICM task assessment method to measure their BD-Metrics. Additional experimental results can be found in Appendix C.3. The experimental findings further support the notion that generative methods contribute to semantic understanding (Yan et al., 2025). However, we also observe that generative codecs perform poorly on fine-grained tasks such as OCRBench, which are well known to yield inferior results on text (Xu et al., 2025).

Table 2: Comparison of BD-Metrics for different VLMs across various tasks. The results are computed using each VLM’s uncompressed performance and measure the degree of degradation for the corresponding VLM under different codecs. Best values are shown in red, second-best in blue.

VLM	Metric	JPEG	HM	VTM	ELIC	TCM	MLIC	HiFiC	ILLM	D.EIC	RDEIC	S.Codec
Qwen chat -7B	OCRB	-236.3	-147.9	-137.2	-51.9	<b>-33.8</b>	<b>-33.4</b>	-262.2	-163.7	-310.5	-206.7	-326.1
	GQA	-8.65	-3.10	-3.04	<b>-1.34</b>	-1.48	-1.58	-2.99	-2.17	-1.95	<b>-1.14</b>	-2.04
	POPE	-6.36	-3.01	-3.46	-2.09	-1.90	<b>-1.65</b>	-4.05	-3.12	-3.05	<b>-1.71</b>	-2.66
	MME	-296.9	-167.7	-183.6	-114.5	-98.4	-100.8	-114.9	-90.8	<b>-90.4</b>	<b>-36.1</b>	-101.9
	MMB	-11.74	-3.91	-5.08	-3.95	<b>-3.12</b>	-3.72	-7.50	-4.15	-6.95	<b>-2.75</b>	-4.82
	SEEDB	-9.91	-4.44	-4.29	-2.04	<b>-2.01</b>	-2.17	-4.89	-3.00	-2.30	<b>-0.99</b>	-2.56
	COCOC	-26.79	-11.12	-11.53	-6.78	-6.01	-6.74	-11.05	-7.90	-5.78	<b>-2.45</b>	<b>-5.76</b>
Intern VL3 -8B	OCRB	-319.9	-239.7	-243.6	-117.1	<b>-102.1</b>	<b>-107.5</b>	-495.6	-333.5	-615.4	-408.5	-670.1
	GQA	-9.57	-6.02	-5.64	<b>-3.15</b>	-3.46	-3.23	-5.02	-3.87	-3.28	<b>-2.09</b>	-4.02
	POPE	-7.33	-3.63	-3.82	-2.75	-2.72	<b>-2.33</b>	-6.55	-4.84	-5.10	<b>-2.60</b>	-4.84
	MME	-266.8	-172.9	-151.5	-95.4	<b>-89.0</b>	<b>-91.9</b>	-231.0	-132.8	-173.6	-92.8	-175.3
	MMB	-11.69	-5.83	-5.74	<b>-3.34</b>	<b>-3.41</b>	-3.48	-11.89	-5.74	-13.48	-5.87	-9.59
	SEEDB	-10.06	-5.72	-5.55	-2.80	<b>-2.62</b>	-2.88	-6.38	-4.44	-4.00	<b>-1.78</b>	-4.22
Qwen VL2.5 -7B	OCRB	-334.6	-231.8	-241.9	-86.5	<b>-82.3</b>	<b>-83.8</b>	-509.9	-317.3	-601.4	-399.6	-662.1
	GQA	-13.28	-7.94	-7.57	-4.98	-4.87	-5.06	-6.37	-4.88	<b>-4.77</b>	<b>-3.21</b>	-4.77
	POPE	-18.38	-9.15	-9.00	<b>-6.04</b>	-6.11	-6.15	-11.48	-8.78	-8.65	<b>-6.10</b>	-8.97
	MME	-522.2	-295.9	-311.0	-162.6	-165.1	-169.4	-231.9	<b>-161.0</b>	-184.6	<b>-93.5</b>	-220.6
	MMB	-24.71	-7.88	-8.17	<b>-3.57</b>	<b>-3.76</b>	-3.77	-11.80	-6.49	-12.58	-5.66	-8.35
	SEEDB	-18.00	-8.94	-8.04	-4.01	-3.85	<b>-3.83</b>	-7.82	-5.16	-4.29	<b>-2.17</b>	-4.49
Janus -pro -7B	OCRB	-259.2	-175.4	-186.1	<b>-84.9</b>	-86.4	<b>-85.9</b>	-312.5	-205.5	-380.2	-246.0	-413.4
	GQA	-7.16	-3.61	-3.28	-1.84	-1.80	<b>-1.50</b>	-2.81	-2.42	-2.17	<b>-1.03</b>	-2.46
	POPE	-22.79	-13.60	-13.48	-7.80	-8.95	-7.62	-7.43	-5.99	<b>-5.50</b>	<b>-3.91</b>	-7.69
	MME	-264.1	-199.6	-166.4	<b>-100.6</b>	-103.7	-104.1	-187.5	-120.3	-137.6	<b>-61.1</b>	-142.6
	MMB	-10.77	-5.52	-4.94	<b>-2.78</b>	<b>-2.77</b>	-3.08	-9.70	-5.49	-9.36	-3.39	-7.44
	SEEDB	-7.16	-4.83	-4.31	<b>-1.96</b>	-2.09	-2.00	-4.96	-3.80	-2.99	<b>-1.61</b>	-3.07

**Finding4: The scaling laws for generalization to unseen input don’t apply to compressed images.** We conduct scaling law experiments across three codec types and multiple tasks, measuring the performance drop between compressed and uncompressed inputs for models of varying sizes, as shown in Figure 5. Our findings reveal that increasing model size does not consistently reduce compression-induced degradation, indicating a gap between model generalization and robustness to distortion, thus breaking the expected scaling law. Additionally, for StableCodec, the highest bitrate does not yield optimal POPE scores in smaller models, though this effect diminishes as model size

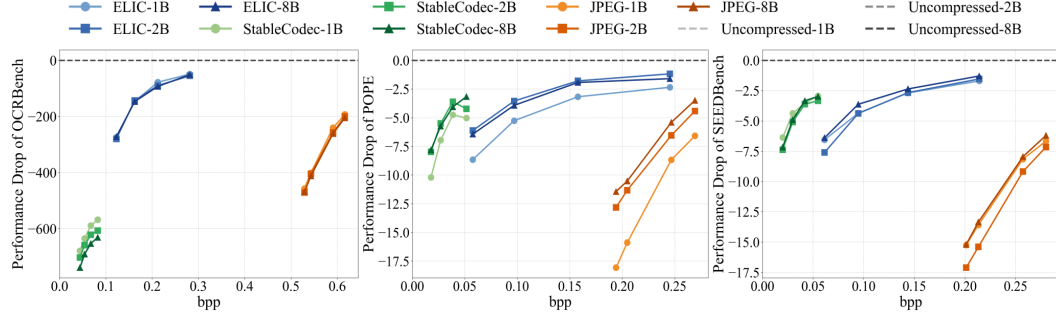


Figure 5: Rate–Metric curves validating the scaling law of distortion robustness are presented for the InternVL3 series models with 1B, 2B, and 8B parameters. Distortion robustness is assessed using OCRBench, POPE, and SEEDBench performance drop relative to the uncompressed results.

grows. This suggests that VLM generalization capacity modulates the rate-distortion behavior of compression, affecting its monotonicity. Further results are available in Appendix C.4.

#### **Finding5: VLM vision tasks correlate with human vision**

**pixel-level metrics, but a gap remains.** To investigate the relationship between human vision and machine perception, we conducted a comparative analysis of VLMs on compressed images using both task-level benchmarks and pixel-level image quality metrics in Figure 6. Specifically, we evaluated VLM performance across multiple downstream tasks while simultaneously measuring image fidelity using perceptual metrics including PSNR, LPIPS, DISTs, and FID. As shown in our results, high pixel-level scores do not always translate to strong VLM task performance, suggesting a decoupling between low-level image quality and semantic understanding. For fine-grained tasks such as OCRBench, pixel-level metrics like PSNR exhibit stronger correlation, while other perceptual metrics show weaker alignment. In contrast, for coarse-grained tasks, perceptual metrics demonstrate higher correlation, though a noticeable gap still remains. This highlights a nuanced gap between human-centric perceptual metrics and machine vision capabilities, and underscores the need for task-aware evaluation protocols when optimizing image compression for machine vision.

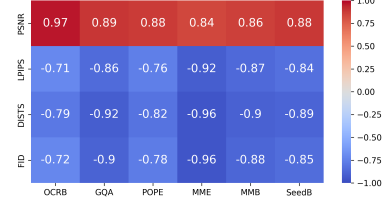


Figure 6: Correlation matrix between human-vision metrics and VLM vision tasks.

## 3 UNDERSTANDING THE PERFORMANCE GAP

In this section, we decompose the performance gap between compressed and uncompressed image into two parts: a). The information gap which is caused by the loss of actual information during image compression; b). The generalization gap which is caused by the VLM’s failure to generalize compressed images. We discuss the decomposition in detail and visualize those two gaps using numerical examples.

### 3.1 THE INFORMATION GAP AND GENERALIZATION GAP

Denote the original image as  $X$ , the compressed image as  $\hat{X}$ , the parameter of VLM as  $\theta$  and the benchmark performance as  $\mathcal{L}(\cdot, \cdot)$ . Then we can decompose the performance gap between compressed image  $\hat{X}$  and uncompressed image  $X$  into two parts:

$$\underbrace{\mathcal{L}(X, \theta) - \mathcal{L}(\hat{X}, \theta)}_{\text{performance gap}} = \underbrace{\mathcal{L}(X, \theta) - \mathcal{L}(\hat{X}, \theta^*)}_{\text{information gap}} + \underbrace{\mathcal{L}(\hat{X}, \theta^*) - \mathcal{L}(\hat{X}, \theta)}_{\text{generalization gap}},$$

where  $\mathcal{L}(\hat{X}, \theta^*) = \max_{\theta} \mathcal{L}(\hat{X}, \theta)$ . (1)

We name the first part information gap. It is defined as the part of performance gap that can not be resolved no matter how the VLM is finetuned. It is the amount of information about the task

that is already lost in image compression process. Given already compressed image  $\hat{X}$ , there is no remedy to information gap. And the information gap has to be solved by improving the compression algorithm.

We name the second part generalization gap. It is defined as the part of performance gap that is caused by VLM’s generalization failure to compressed image. The generalization gap can be reduced by finetuning the VLM using compressed images. In Sec. 4, we propose a VLM adaptor to reduce generalization gap for different image compressors and bitrates.

### 3.2 VISUALIZATION WITH JPEG COMPRESSOR

To better understand the information gap and generalization gap, we provide a numerical example in Table 3. More specifically, we finetune VLM parameter  $\theta$  for JPEG, ELIC and ILLM respectively. The reducible gap is generation gap, and the irreducible gap is information gap.

Table 3: The information and generalization gap on SEEDBench and POPE, with JPEG, ILLM and ELIC as codecs.

	SEEDBench			POPE		
	JPEG	ELIC	ILLM	JPEG	ELIC	ILLM
uncompressed $\mathcal{L}(X, \theta)$				73.81		86.21
compressed $\mathcal{L}(\hat{X}, \theta)$	60.56	65.28	56.13	49.92	76.41	61.4
compressed finetune $\mathcal{L}(\hat{X}, \theta^*)$	64.31	69.48	58.55	79.40	82.31	74.02
Performance gap	13.25	8.53	17.68	36.29	9.8	24.81
Information gap	9.5	4.33	15.26	6.81	3.9	12.19
Generalization gap	3.75	4.2	2.42	29.48	5.9	12.62

## 4 CLOSING GENERALIZATION GAP WITH VLM ADAPTOR

### 4.1 PROPOSED METHOD

Based on the analysis in Section 3, we propose a unified VLM adaptor that can adapt to different types of compression distortions and close the generalization gap. Since fine-tuning the entire VLM requires substantial computational resources, incurs high costs, and is challenging to implement, we found that fine-tuning only the VLM encoder can still yield significant performance gains.

Specifically, existing VLM vision encoders are generally based on the Vision Transformers (ViT) architecture (Han et al., 2022). We need to enable the encoder to understand the distortion types and corresponding compression levels of the compressed images, and incorporate this information as conditional input to the encoder. Assuming there are  $m$  existing codecs with different types of distortion, each with  $n$  compression levels, we first perform one-hot encoding for each compressor and then map it to the latent variable space through an embedding layer  $T(\cdot)$  to get the codec condition embedding  $C_{\text{emb}}$ , as follows:

$$C_{\text{emb}} = T(m, n, d), \quad (2)$$

where  $d$  indicates the embedding dimension aligning with the VLM vision encoder. To ensure that the entire VLM vision encoder can incorporate the codec condition at all positions, we refer to the fusion methods of conditional embedding and time embedding in conditional diffusion models (Rombach et al., 2022; Preechakul et al., 2022), and add the codec condition  $C_{\text{emb}}$  to the rotary positional embedding (RoPE) (Su et al., 2024) in vision encoder, yielding the new conditional positional embedding.

Based on this, we can train the VLM’s unified conditional vision encoder (CVE) with parameter  $\theta^*$  using compressed images to distill the original vision encoder (VE) with parameter  $\theta$ , ensuring that the features extracted from uncompressed images  $X$  through VE are as similar as possible to the features extracted from compressed images  $\hat{X}$  through CVE. To achieve this, we introduce the

following distillation loss  $\mathcal{L}_d$ , which aims to minimize the mean squared error (MSE) between the two output features:

$$\mathcal{L}_d = \|\text{CVE}(\hat{X}, C_{\text{emb}}, \theta^*) - \text{VE}(X, \theta)\|_2^2. \quad (3)$$

This approach aims to bridge the gap between compressed visual features and the original domain, fine-tuning the VLM to reduce the generalization gap. This distinguishes our method from existing works in the field of coding for machines that focus on fine-tuning for specific codecs.

#### 4.2 EXPERIMENTAL SETTING

To show our enhancement effect, we utilize Qwen-VL2.5-3B and InternVL3-1B as our VLM model and select one representative codec from each of the three compression distortion methods listed in Table 1, namely JPEG, ELIC, and ILLM, aligning with Table 3. We used four bitrate levels for training, resulting in a 12-dimensional codec conditional embedding. For the training dataset, we used COCO, which contains more than 11w images. These images were compressed with different bitrates from the three codecs mentioned above, creating a training set containing a large number of compressed images. To validate the generalization capability of our proposed method, we conducted experiments on previously unseen compressed-distortion images such as HM, MLICpp, and DiffEIC, directly applying the enhanced vision encoder introduced in this work for compression. In addition, we performed comparative and analytical experiments on image coding for machines, which further demonstrate the effectiveness of the information gap and generalization gap.

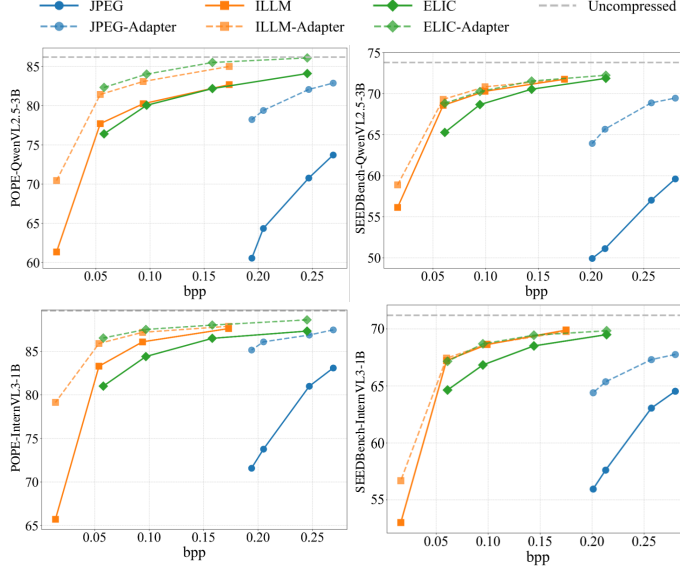


Figure 7: Rate-accuracy comparison on POPE and SEEDBench using QwenVL2.5-3B and InternVL3-1B.

#### 4.3 EXPERIMENTAL RESULTS

**Quantitative Results.** To quantitatively evaluate the effectiveness of our adapter-enhanced compression methods, we perform rate–accuracy analysis on two representative VLMs, QwenVL2.5-3B and InternVL3-1B. Their performance is evaluated on the coarse-grained benchmark POPE and the fine-grained benchmark SEEDBench, while additional results on OCRBench, MME, GQA, and MBMbench are provided in Appendix D. As shown in Figure 7, across all tested bitrates, adapter variants consistently outperform their corresponding base codecs, demonstrating superior robustness under compression. Notably, JPEG-Adapter achieves substantial improvements on both metrics, with gains of approximately 30% at low bitrate. Additionally, ELIC and ILLM show over 10% improvement on the POPE metric. Furthermore, BD-Metric results in Table 4 reinforce these findings. Compared to the original VLM model without the adapter, our method achieves a performance gain of over 12 units on two metrics for JPEG at the same bitrate for QwenVL2.5-3B, with also signifi-

Table 4: The BD-Metric results are compared against the original compression outcomes using QwenVL2.5-3B and InternVL3-1B, where BD-P refers to BD-POPE and BD-S refers to BD-SEEDBench.

VLM	Codec	BD-P	BD-S
Qwen VL2.5 -3B	JPEG	12.62	12.88
	ELIC	3.42	0.69
	ILLM	3.52	1.23
Intern VL3 -1B	JPEG	8.36	5.62
	ELIC	2.19	1.19
	ILLM	2.45	0.42

cant improvements on ELIC and ILLM. These results collectively validate the effectiveness of our strategy in preserving semantic fidelity and benchmark performance under aggressive compression.

**Qualitative Results.** To evaluate robustness under compression artifacts, we conducted qualitative comparisons based on QwenVL2.5-3B as shown in Figure 8. Standard VLMs showed significant performance drops, often misinterpreting key visual cues. In contrast, our method consistently produced correct predictions, demonstrating strong resilience to compression-induced distortions. These results suggest that our approach enables reliable multimodal understanding even under heavy lossy compression, making it well-suited for deployment in bandwidth-constrained scenarios.

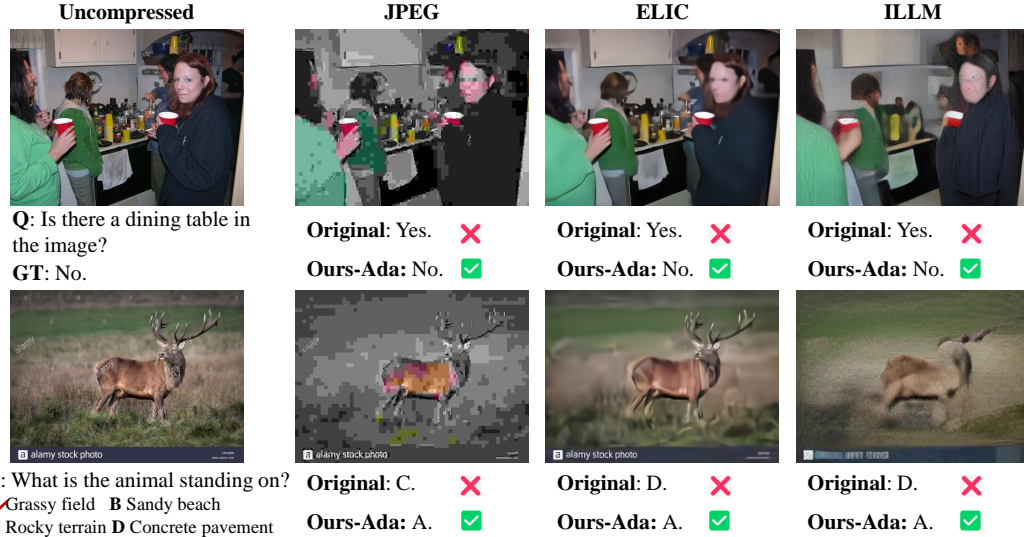


Figure 8: Subjective results for POPE and SEEDBench metrics of standard VLM and our method.

**Generalization Results.** To test the performance on unseen codec, we evaluate HM, MLICpp, and DiffEIC using our already-trained adaptor, pretending they are JPEG, ELIC, and MS-ILLM respectively. The experimental results are shown in Figure 9 and Table 5. From the curves and BD-Metric results, we observe that the adaptor yields consistent improvements on all unselected codecs, even though these codecs were never seen during training. Notably, MLICpp achieves larger gains than ELIC itself on SEEDBench, which is both interesting and unexpected. We also notice that DiffEIC improves on POPE but exhibits a very slight drop on SEEDBench. This may be attributed to the fact that MS-ILLM is a GAN-based codec, whereas DiffEIC is a diffusion-based codec, leading to a larger semantic and structural gap between the two codec families.

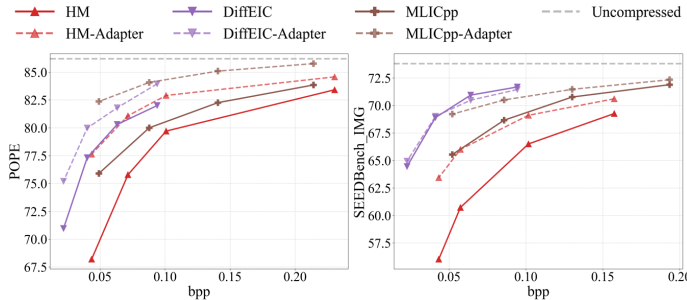


Figure 9: Rate-accuracy comparison on POPE and SEEDBench using QwenVL2.5-3B.

Table 5: The BD-Metric results are compared against the original compression outcomes, where BD-P refers to BD-POPE and BD-S refers to BD-SEEDBench.

Codec	BD-P	BD-S
HM	2.98	3.12
MLICpp	3.32	1.22
DiffEIC	2.15	-0.16

**Comparison with ICM.** Our enhancement method shares the same objective as ICM which improves the robustness to compressed images but from different prospective of information and generalization gap. To better illustrate the gap identified in this work, we conducted evaluations of TransTIC (Chen et al., 2023b) on the POPE dataset, as shown in Table 6. First, we tested the results

Table 6: The BD-Metric results are compared with ICM methods to visualize the two gaps.

Codec	TIC	TransTIC	TIC-Adapter	TransTIC-Adapter
BD-POPE	0.00	0.18	2.43	<b>3.02</b>

of the base codec TIC (Lu et al., 2022) and fine-tuned the TransTIC with VLM vision encoder to reduce the information gap. We then applied the enhancement method to both models and found that simultaneously addressing both the generalization and information gap yields the best results.

## 5 RELATED WORKS

**Image Coding for Humans.** In recent years, deep learning has significantly advanced image compression, surpassing traditional hand-crafted codecs. Existing methods can be grouped into three categories: traditional, learning-based, and generative compression. Traditional codecs, from JPEG (Wallace, 1991) to HEVC (Sullivan et al., 2012) and VVC (Bross et al., 2021), have steadily improved but at the cost of increasing computational complexity, eventually reaching a plateau. Learning-based compression methods began to emerge and have progressively incorporated state-of-the-art network architectures, such as ResNet (Cheng et al., 2020), Transformers (Liu et al., 2023a) and Mamba (Zeng et al., 2025), as well as entropy modeling along both channel and spatial dimensions (Minnen et al., 2018; He et al., 2022; Jiang et al., 2023), achieving superior compression performance compared to traditional codecs. Nevertheless, due to their pixel-level optimization, learning-based methods often produce poor visual quality at extremely low bitrates, which is undesirable for human perception. To address this, generative model-based approaches, including those leveraging GANs (Mentzer et al., 2020; Muckley et al., 2023) and Diffusion models (Li et al., 2024c; 2025; Zhang et al., 2025a), have been developed to optimize compression with respect to perceptual quality. However, they remain computationally intensive and large in size, limiting practical deployment and leaving considerable room for improvement.

**Image Coding for Machines.** With the rapid development of computer vision and the widespread adoption of intelligent tasks, compression techniques tailored for machine vision have been extensively investigated. In response, the Moving Picture Experts Group (MPEG) established Video Coding for Machines (VCM) (Kang et al., 2022) and Feature Coding for Machines (FCM) (Rosewarne, 2023). Existing methods (Zhang et al., 2024b; Kim et al., 2023; Liu et al., 2023b; Zhang et al., 2024a; Li et al., 2024b; Chen et al., 2023b) mainly focus on specific architectures, such as Fast-RCNN (Ren et al., 2015) and Mask-RCNN (He et al., 2017), and target particular tasks like object detection, instance segmentation, and object tracking, with limited generalization capabilities. Furthermore, driven by the recent success of VLMs and their increasingly broad applications, some studies (Kao et al., 2024; Li et al., 2024a) have begun exploring image compression for VLMs. However, these works typically focus on a single codec and lack a comprehensive benchmark like image compression for human vision (Hu et al., 2021).

**Vision-Language Models.** VLMs are large-scale models that integrate visual modalities with language understanding Zhan et al. (2024); Chen et al. (2025). In recent years, there has been a surge in research utilizing VLMs (Wang et al., 2024; Chen et al., 2024; Zhu et al., 2025; Yao et al., 2024; Team et al., 2025) for tasks such as image understanding, image recognition, instance segmentation, and object detection, significantly enhancing the model’s generalization capabilities. To evaluate the comprehensive performance of VLMs, several benchmark studies have been proposed, including SEEDBench (Li et al., 2023a), MMBench (Liu et al., 2024a), MME (Chaoyou et al., 2023), OCR-Bench Liu et al. (2024b) and et al. However, the existing evaluation datasets consist of high-bitrate, clear images, and there has been little exploration of methods for evaluating VLM performance on compressed images, which are of great importance as they can significantly save bandwidth and resources.

## 6 CONCLUSION

In this paper, we present a comprehensive benchmark for evaluating VLMs on heavily compressed images, covering over one million samples and assessing both coarse-grained and fine-grained met-

rics. Our analysis reveals that existing VLMs struggle under compression, and we attribute this to two distinct factors: an inherent information gap due to irreversible data loss, and a generalization gap stemming from poor adaptation to distorted inputs. While the former is difficult to mitigate, we show that the latter can be addressed through model design. To this end, we propose a lightweight VLM adaptor that significantly improves performance across diverse codecs and bitrates. Empirical results demonstrate strong gains in recognition accuracy, highlighting the adaptor’s potential for real-world deployment. We acknowledge that our current experiments do not include the latest proprietary VLM models due to API cost constraints, but we plan to extend our study in future work. We believe this research may contribute to the advancement of image coding for machines and semantic compression.

## ETHICS STATEMENT

This work focuses on benchmarking and enhancing vision-language models (VLMs) for compressed image understanding. Since the proposed models do not generate novel content, ethical concerns are relatively limited. However, VLMs may still exhibit hallucination issues, such as factual inaccuracies and reduced reliability in certain outputs.

## REPRODUCIBILITY STATEMENT

All experimental results are documented in the appendix. For empirical validation, we utilize publicly available datasets. Detailed implementation settings and hyperparameter configurations are also provided in the appendix to facilitate reproducibility.

## REFERENCES

- Jinze Bai, Shuai Bai, Yunfei Chu, Zeyu Cui, Kai Dang, Xiaodong Deng, Yang Fan, Wenbin Ge, Yu Han, Fei Huang, et al. Qwen technical report. *arXiv preprint arXiv:2309.16609*, 2023.
- Shuai Bai, Keqin Chen, Xuejing Liu, Jialin Wang, Wenbin Ge, Sibo Song, Kai Dang, Peng Wang, Shijie Wang, Jun Tang, et al. Qwen2. 5-vl technical report. *arXiv preprint arXiv:2502.13923*, 2025.
- J. Ballé, D. Minnen, S. Singh, S. Hwang, and N. Johnston. Variational image compression with a scale hyperprior. *arXiv preprint arXiv:1802.01436*, 2018.
- B. Bross, Y. Wang, Y. Ye, S. Liu, J. Chen, G. Sullivan, and J. Ohm. Overview of the versatile video coding (VVC) standard and its applications. *IEEE TCSVT*, 31(10):3736–3764, 2021.
- Fu Chaoyou, Chen Peixian, Shen Yunhang, Qin Yulei, Zhang Mengdan, Lin Xu, Yang Jinrui, Zheng Xiawu, Li Ke, Sun Xing, et al. Mme: A comprehensive evaluation benchmark for multimodal large language models. *arXiv preprint arXiv:2306.13394*, 3, 2023.
- Chaoran Chen, Mai Xu, Shengxi Li, Tie Liu, Minglang Qiao, and Zhuoyi Lv. Residual based hierarchical feature compression for multi-task machine vision. In *2023 IEEE International Conference on Multimedia and Expo (ICME)*, pp. 1463–1468. IEEE, 2023a.
- Xiaokang Chen, Zhiyu Wu, Xingchao Liu, Zizheng Pan, Wen Liu, Zhenda Xie, Xingkai Yu, and Chong Ruan. Janus-pro: Unified multimodal understanding and generation with data and model scaling. *arXiv preprint arXiv:2501.17811*, 2025.
- Xinlei Chen, Hao Fang, Tsung-Yi Lin, Ramakrishna Vedantam, Saurabh Gupta, Piotr Dollár, and C Lawrence Zitnick. Microsoft coco captions: Data collection and evaluation server. *arXiv preprint arXiv:1504.00325*, 2015.
- Yi-Hsin Chen, Ying-Chieh Weng, Chia-Hao Kao, Cheng Chien, Wei-Chen Chiu, and Wen-Hsiao Peng. Transtic: Transferring transformer-based image compression from human perception to machine perception. In *Proceedings of the IEEE/CVF International Conference on Computer Vision*, pp. 23297–23307, 2023b.

- Zhe Chen, Jiannan Wu, Wenhui Wang, Weijie Su, Guo Chen, Sen Xing, Muyan Zhong, Qinglong Zhang, Xizhou Zhu, Lewei Lu, et al. Internvl: Scaling up vision foundation models and aligning for generic visual-linguistic tasks. In *Proceedings of the IEEE/CVF conference on computer vision and pattern recognition*, pp. 24185–24198, 2024.
- Z. Cheng, H. Sun, M. Takeuchi, and J. Katto. Learned image compression with discretized gaussian mixture likelihoods and attention modules. In *IEEE CVPR*, pp. 7939–7948, 2020.
- Haodong Duan, Junming Yang, Yuxuan Qiao, Xinyu Fang, Lin Chen, Yuan Liu, Xiaoyi Dong, Yuhang Zang, Pan Zhang, Jiaqi Wang, et al. Vlmevalkit: An open-source toolkit for evaluating large multi-modality models. In *Proceedings of the 32nd ACM international conference on multimedia*, pp. 11198–11201, 2024.
- Yongchao Feng, Yajie Liu, Shuai Yang, Wenrui Cai, Jinqing Zhang, Qiqi Zhan, Ziyue Huang, Hongxi Yan, Qiao Wan, Chenguang Liu, et al. Vision-language model for object detection and segmentation: A review and evaluation. *arXiv preprint arXiv:2504.09480*, 2025.
- Kai Han, Yunhe Wang, Hanting Chen, Xinghao Chen, Jianyuan Guo, Zhenhua Liu, Yehui Tang, An Xiao, Chunjing Xu, Yixing Xu, et al. A survey on vision transformer. *IEEE transactions on pattern analysis and machine intelligence*, 45(1):87–110, 2022.
- Dailan He, Ziming Yang, Weikun Peng, Rui Ma, Hongwei Qin, and Yan Wang. Elic: Efficient learned image compression with unevenly grouped space-channel contextual adaptive coding. In *Proceedings of the IEEE/CVF conference on computer vision and pattern recognition*, pp. 5718–5727, 2022.
- K. He, G. Gkioxari, P. Dollár, and R. Girshick. Mask R-CNN. In *IEEE ICCV*, pp. 2961–2969, 2017.
- Yueyu Hu, Wenhan Yang, Zhan Ma, and Jiaying Liu. Learning end-to-end lossy image compression: A benchmark. *IEEE Transactions on Pattern Analysis and Machine Intelligence*, 44(8):4194–4211, 2021.
- Drew A Hudson and Christopher D Manning. Gqa: A new dataset for real-world visual reasoning and compositional question answering. In *Proceedings of the IEEE/CVF conference on computer vision and pattern recognition*, pp. 6700–6709, 2019.
- Wei Jiang, Jiayu Yang, Yongqi Zhai, Feng Gao, and Ronggang Wang. Mlic++: Linear complexity multi-reference entropy modeling for learned image compression. *arXiv preprint arXiv:2307.15421*, 2023.
- J. Kang, H. Jeong, S. Bae, H. Kim, K. Kim, and S. Jeong. Feature compression with resize in feature domain. In *ISO/IEC JTC 1/SC 29/WG 2 m59537*, 2022.
- Chia-Hao Kao, Cheng Chien, Yu-Jen Tseng, Yi-Hsin Chen, Alessandro Gnutti, Shao-Yuan Lo, Wen-Hsiao Peng, and Riccardo Leonardi. Bridging compressed image latents and multimodal large language models. *arXiv preprint arXiv:2407.19651*, 2024.
- Yeongwoong Kim, Hyewon Jeong, Janghyun Yu, Younhee Kim, Jooyoung Lee, Se Yoon Jeong, and Hui Yong Kim. End-to-end learnable multi-scale feature compression for vcm. *IEEE Transactions on Circuits and Systems for Video Technology*, 34(5):3156–3167, 2023.
- Binzhe Li, Shurun Wang, Shiqi Wang, and Yan Ye. High efficiency image compression for large visual-language models. *IEEE Transactions on Circuits and Systems for Video Technology*, 2024a.
- Bohao Li, Rui Wang, Guangzhi Wang, Yuying Ge, Yixiao Ge, and Ying Shan. Seed-bench: Benchmarking multimodal llms with generative comprehension. *arXiv preprint arXiv:2307.16125*, 2023a.
- Han Li, Shaohui Li, Shuangrui Ding, Wenrui Dai, Maida Cao, Chenglin Li, Junni Zou, and Hongkai Xiong. Image compression for machine and human vision with spatial-frequency adaptation. In *European Conference on Computer Vision*, pp. 382–399. Springer, 2024b.
- Yifan Li, Yifan Du, Kun Zhou, Jinpeng Wang, Wayne Xin Zhao, and Ji-Rong Wen. Evaluating object hallucination in large vision-language models. *arXiv preprint arXiv:2305.10355*, 2023b.

- Zhiyuan Li, Yanhui Zhou, Hao Wei, Chenyang Ge, and Jingwen Jiang. Towards extreme image compression with latent feature guidance and diffusion prior. *IEEE Transactions on Circuits and Systems for Video Technology*, 2024c.
- Zhiyuan Li, Yanhui Zhou, Hao Wei, Chenyang Ge, and Ajmal Mian. Rdeic: Accelerating diffusion-based extreme image compression with relay residual diffusion. *IEEE Transactions on Circuits and Systems for Video Technology*, 2025.
- Jinming Liu, Heming Sun, and Jiro Katto. Learned image compression with mixed transformer-cnn architectures. In *Proceedings of the IEEE/CVF conference on computer vision and pattern recognition*, pp. 14388–14397, 2023a.
- Tie Liu, Mai Xu, Shengxi Li, Chaoran Chen, Li Yang, and Zhuoyi Lv. Learnt mutual feature compression for machine vision. In *IEEE ICASSP 2023*, pp. 1–5. IEEE, 2023b.
- Yuan Liu, Haodong Duan, Yuanhan Zhang, Bo Li, Songyang Zhang, Wangbo Zhao, Yike Yuan, Jiaqi Wang, Conghui He, Ziwei Liu, et al. Mmbench: Is your multi-modal model an all-around player? In *European conference on computer vision*, pp. 216–233. Springer, 2024a.
- Yuliang Liu, Zhang Li, Mingxin Huang, Biao Yang, Wenwen Yu, Chunyuan Li, Xu-Cheng Yin, Cheng-Lin Liu, Lianwen Jin, and Xiang Bai. Ocrbench: on the hidden mystery of ocr in large multimodal models. *Science China Information Sciences*, 67(12):220102, 2024b.
- Guo Lu, Wanli Ouyang, Dong Xu, Xiaoyun Zhang, Chunlei Cai, and Zhiyong Gao. Dvc: An end-to-end deep video compression framework. In *Proceedings of the IEEE/CVF conference on computer vision and pattern recognition*, pp. 11006–11015, 2019.
- Ming Lu, Peiyao Guo, Huiqing Shi, Chunlong Cao, and Zhan Ma. Transformer-based image compression. In *2022 Data Compression Conference (DCC)*, pp. 469–469, 2022. doi: 10.1109/DCC52660.2022.00080.
- Fabian Mentzer, George D Toderici, Michael Tschannen, and Eirikur Agustsson. High-fidelity generative image compression. *Advances in neural information processing systems*, 33:11913–11924, 2020.
- David Minnen, Johannes Ballé, and George D Toderici. Joint autoregressive and hierarchical priors for learned image compression. *Advances in neural information processing systems*, 31, 2018.
- Matthew J Muckley, Alaaeldin El-Nouby, Karen Ullrich, Hervé Jégou, and Jakob Verbeek. Improving statistical fidelity for neural image compression with implicit local likelihood models. In *International Conference on Machine Learning*, pp. 25426–25443. PMLR, 2023.
- Konpat Preechakul, Nattanat Chatthee, Suttisak Wizadwongsa, and Supasorn Suwajanakorn. Diffusion autoencoders: Toward a meaningful and decodable representation. In *Proceedings of the IEEE/CVF conference on computer vision and pattern recognition*, pp. 10619–10629, 2022.
- S. Ren, K. He, R. Girshick, and J. Sun. Faster R-CNN: Towards real-time object detection with region proposal networks. *NIPS*, 28, 2015.
- Robin Rombach, Andreas Blattmann, Dominik Lorenz, Patrick Esser, and Björn Ommer. High-resolution image synthesis with latent diffusion models. In *Proceedings of the IEEE/CVF conference on computer vision and pattern recognition*, pp. 10684–10695, 2022.
- C. Rosewarne. Proposed common test conditions for feature compression for video coding for machines. In *ISO/IEC JTC 1/SC 29/WG 4 m65749*, 2023.
- Jianlin Su, Murtadha Ahmed, Yu Lu, Shengfeng Pan, Wen Bo, and Yunfeng Liu. Roformer: Enhanced transformer with rotary position embedding. *Neurocomputing*, 568:127063, 2024.
- G. Sullivan, J. Ohm, W. Han, and T. Wiegand. Overview of the high efficiency video coding (hevc) standard. *IEEE Transactions on circuits and systems for video technology*, 22(12):1649–1668, 2012.

- Gemma Team, Aishwarya Kamath, Johan Ferret, Shreya Pathak, Nino Vieillard, Ramona Merhej, Sarah Perrin, Tatiana Matejovicova, Alexandre Ramé, Morgane Rivière, et al. Gemma 3 technical report. *arXiv preprint arXiv:2503.19786*, 2025.
- Gregory K Wallace. The JPEG still picture compression standard. *Communications of the ACM*, 34(4):30–44, 1991.
- Peng Wang, Shuai Bai, Sinan Tan, Shijie Wang, Zhihao Fan, Jinze Bai, Keqin Chen, Xuejing Liu, Jialin Wang, Wenbin Ge, et al. Qwen2-vl: Enhancing vision-language model’s perception of the world at any resolution. *arXiv preprint arXiv:2409.12191*, 2024.
- Tongda Xu, Jiahao Li, Bin Li, Yan Wang, Ya-Qin Zhang, and Yan Lu. Picd: Versatile perceptual image compression with diffusion rendering. In *Proceedings of the Computer Vision and Pattern Recognition Conference*, pp. 28436–28445, 2025.
- Zhiyuan Yan, Kaiqing Lin, Zongjian Li, Junyan Ye, Hui Han, Zhendong Wang, Hao Liu, Bin Lin, Hao Li, Xue Xu, et al. Can understanding and generation truly benefit together—or just coexist? *arXiv preprint arXiv:2509.09666*, 2025.
- Yuan Yao, Tianyu Yu, Ao Zhang, Chongyi Wang, Junbo Cui, Hongji Zhu, Tianchi Cai, Haoyu Li, Weilin Zhao, Zihui He, et al. Minicpm-v: A gpt-4v level mllm on your phone. *arXiv preprint arXiv:2408.01800*, 2024.
- Xiang Yue, Yuansheng Ni, Kai Zhang, Tianyu Zheng, Ruoqi Liu, Ge Zhang, Samuel Stevens, Dongfu Jiang, Weiming Ren, Yuxuan Sun, et al. Mmmu: A massive multi-discipline multi-modal understanding and reasoning benchmark for expert agi. In *Proceedings of the IEEE/CVF Conference on Computer Vision and Pattern Recognition*, pp. 9556–9567, 2024.
- Fanhу Zeng, Hao Tang, Yihua Shao, Siyu Chen, Ling Shao, and Yan Wang. Mambaic: State space models for high-performance learned image compression. In *Proceedings of the Computer Vision and Pattern Recognition Conference*, pp. 18041–18050, 2025.
- Jun Zhan, Junqi Dai, Jiasheng Ye, Yunhua Zhou, Dong Zhang, Zhigeng Liu, Xin Zhang, Ruibin Yuan, Ge Zhang, Linyang Li, et al. Anygpt: Unified multimodal llm with discrete sequence modeling. *arXiv preprint arXiv:2402.12226*, 2024.
- Tianyu Zhang, Xin Luo, Li Li, and Dong Liu. Stablecodec: Taming one-step diffusion for extreme image compression. *arXiv preprint arXiv:2506.21977*, 2025a.
- Yuan Zhang, Hanming Wang, Yunlong Li, and Lu Yu. Afc: Asymmetrical feature coding for multi-task machine intelligence. In *2024 IEEE International Conference on Multimedia and Expo Workshops (ICMEW)*, pp. 1–6. IEEE, 2024a.
- Zifu Zhang, Shengxi Li, Tie Liu, Mai Xu, Tao Xu, Zhenyu Guan, and Zhuoyi Lv. Hybrid single input and multiple output method for compressing features towards machine vision tasks. In *2024 IEEE International Conference on Image Processing (ICIP)*, pp. 1870–1876. IEEE, 2024b.
- Zifu Zhang, Shengxi Li, Henan Liu, Mai Xu, and Ce Zhu. Continuous patch stitching for block-wise image compression. *IEEE Signal Processing Letters*, 2025b.
- Jinguo Zhu, Weiyun Wang, Zhe Chen, Zhaoyang Liu, Shenglong Ye, Lixin Gu, Hao Tian, Yuchen Duan, Weijie Su, Jie Shao, et al. Internvl3: Exploring advanced training and test-time recipes for open-source multimodal models. *arXiv preprint arXiv:2504.10479*, 2025.

## A DETAILED BENCHMARK SETTING.

In this section, we provide the detailed codec parameters as shown in Table 7. Our primary focus is to evaluate VLM performance on compressed images under low bitrate conditions; therefore, we selected configurations that yield a bits-per-pixel (bpp) below 0.3. For learning-based and generative codecs, we primarily adopt the pretrained models released by their respective papers. However, for certain codecs such as TCM, MLICpp, and HiFiC, whose default bitrate settings do not align with our target range, we fine-tuned the models using their lowest available bitrate configurations.

Additionally, we report the evaluation results of the selected VLMs on uncompressed images in Figure 10, serving as a reference upper bound for each model-task pair. The metrics are computed using a standardized comparison protocol, which may differ slightly from those reported in the original papers. However, we conducted a careful cross-check and found the discrepancies to be minor. Since our focus is on quantifying the degradation caused by compression, the absolute metric values are less critical than the relative performance drop.

Table 7: Three categories of selected image codecs with different bitrate parameters.

Types	Codecs	P.	Value
Traditional Codecs	JPEG	Q	{1, 3, 5, 6}
	HM	QP	{40-50}
	VTM	QP	{40-53}
Learning -based Codecs	ELIC	$\lambda$	$\{4, 8, 16, 32\} \times 10^{-3}$
	TCM	$\lambda$	$\{5, 10, 18, 25\} \times 10^{-4}$
	MLICpp	$\lambda$	$\{4, 9, 18, 35\} \times 10^{-4}$
Generative Codecs	HiFiC	$\lambda$	$\{2, 6, 8, 14\} \times 10^{-2}$
	MS-ILLM	Q	{vlo2, 1, 2, 3}
	DiffEIC	$\lambda$	{2, 4, 8, 16}
	RDEIC	$\lambda_r$	{0.1, 0.5, 1, 2}
S.Codec	$\lambda_t$		{2, 4, 8, 16}

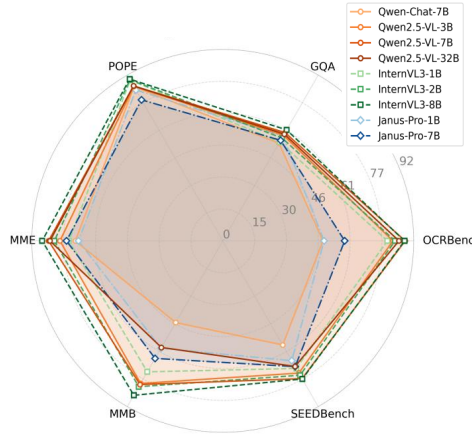


Figure 10: Comparison of VLMs on coarse-grained and fine-grained Benchmarks.

## B DETAILED TASK DESCRIPTION

We systematically evaluate nine state-of-the-art vision–language models (VLMs) on both compressed and uncompressed images using seven complementary metrics. Table 8 summarizes the evaluation design, including the primary focus of each metric, its sub-metrics, and the number of images considered. Detailed discussions are provided in the following subsections.

In each subsection, we further analyze the impact of image compression by considering four representative codecs. For concreteness, we report detailed per-codec results of Qwen-Chat-7B, providing fine-grained evidence of how compression artifacts affect understanding of VLMs.

### B.1 POPE (POLLING-BASED OBJECT PROBING EVALUATION)

We use 5127 images from POPE (Li et al., 2023b), which formulates the evaluation of object hallucination in large VLMs as a binary classification task that prompts LVLMs to output “Yes” or “No”. Questions with the answer “No” are built by sampling from negative objects with three different strategies corresponding to the three metrics based-on F1 score reported below, and the column “Overall” is weighted average of these metrics.

- Random: Randomly sample the objects that do not exist in the image.
- Popular: Select the top-k most frequent objects in the whole image dataset that do not exist in the current image, where k is half of the number of polling questions per image.

Table 8: Comparison of seven widely used multimodal evaluation benchmarks: POPE, OCRBench, COCO-Caption, GQA, MMBench, SEED-Bench, and MME.

Benchmark	Primary Focus	Selected Eval Metrics	Number of Images
POPE	Object hallucination detection	Random, popular and adversarial	5127
COCO-Caption	Image caption generation	CIDEr, ROUGE <sub>L</sub> and BLEU	5000
OCRBench	Effectiveness in text-related visual tasks	Text Recognition, Scene Text-Centric VQA, Document-Oriented VQA, KIE, and HMER	1000
GQA	Visual reasoning and compositional question answering	The structural type including choose, compare, logical, query and verify	398
MME	Perception and cognition abilities	OCR, coarse and fine-grained recognition	1187
MMBench	Robust and holistic, bilingual VLM evaluation	Six L-2 abilities including AR, CP, FP-C, FP-S, LR and RR	4329
SEEDBench	Objective evaluation of MLLMs on generative comprehension	9 dimensions covering image-level and instance-level perception and reasoning	14232

- Adversarial: First rank all objects according to their co-occurring frequencies with the ground-truth objects, and then select the top-k frequent ones that do not exist in the image.

Table 9: Evaluation results of Qwen-Chat-7B on the POPE metric.

Codec	bpp	Overall	Random	Popular	Adversarial
JPEG	0.27	82.32	79.75	83.02	84.33
	0.25	81.09	78.28	83.25	81.91
	0.20	77.10	78.32	74.42	78.71
	0.19	75.69	73.30	77.05	76.84
ELIC	0.25	84.77	82.48	86.85	85.10
	0.16	83.96	85.89	81.76	84.34
	0.10	83.58	83.88	85.64	81.34
	0.06	82.10	82.39	79.82	84.21
MSILLM	0.17	85.52	83.17	87.84	85.68
	0.09	83.96	84.10	86.38	81.53
	0.05	82.17	79.77	84.44	82.43
	0.01	73.05	72.98	70.64	75.70
RDEIC	0.12	84.64	84.85	86.76	82.44
	0.09	85.12	87.19	82.79	85.50
	0.07	84.46	84.98	82.18	86.33
	0.03	81.92	79.55	82.40	83.93

## B.2 COCO-CAPTION

COCO-Caption (Chen et al., 2015) provides a standardized dataset and evaluation protocol for image caption generation using 5000 MS COCO testing images with 40 reference sentences per image. Captions output by different approaches are evaluated by automatic metrics including CIDEr, ROUGE<sub>L</sub> and Bleu.

- CIDEr aggregates Term Frequency Inverse Document Frequency (TF-IDF) weighted n-gram cosine similarity.
- ROUGE<sub>L</sub> computes an F-measure based on the longest common subsequence (LCS) between candidate and reference captions.
- BLEU analyzes the co-occurrences of n-grams between the candidate and reference sentences and computes a corpus-level clipped n-gram precision with a brevity penalty:

$$\text{BLEUK} = \text{BP} \cdot \exp \left( \sum_{k=1}^K w_k \log p_k \right),$$

where  $p_k$  are clipped  $k$ -gram precisions and BP is the brevity penalty.

Table 10: Evaluation results of Qwen-Chat-7B on the COCO-Caption metric.

Codec	bpp	CIDEr	ROUGE <sub>L</sub>	Bleu1	Bleu2	Bleu3	Bleu4
JPEG	0.27	83.09	51.08	71.82	54.20	39.97	29.36
	0.25	78.37	50.32	70.94	52.76	38.51	28.09
	0.20	60.35	45.94	65.12	45.91	32.06	22.49
	0.19	56.37	44.97	63.69	44.31	30.60	21.18
ELIC	0.26	95.73	54.06	75.09	58.01	43.76	32.79
	0.16	93.02	53.67	74.49	57.40	42.97	31.96
	0.10	88.33	52.62	73.46	55.85	41.48	30.75
	0.06	81.56	50.84	71.53	53.49	39.17	28.64
MSILLM	0.17	96.66	54.45	75.37	58.47	44.34	33.43
	0.09	95.20	54.10	75.25	58.32	44.02	33.00
	0.05	90.84	53.35	74.21	57.00	42.66	31.77
	0.01	53.11	44.49	62.79	43.16	29.68	20.61
RDEIC	0.12	97.84	54.66	75.74	58.92	44.78	33.76
	0.09	97.05	54.37	75.55	58.78	44.57	33.56
	0.07	97.00	54.69	75.70	58.91	44.69	33.62
	0.03	89.30	53.00	73.65	56.34	42.16	31.43

### B.3 OCRBENCH

We use 1000 images from OCRBench (Liu et al., 2024b), a comprehensive benchmark assessing Optical Character Recognition (OCR) capabilities in LLMs through five text-related visual tasks including Text Recognition, Scene Text-Centric Visual Question Answering (VQA), Document-Oriented VQA, Key Information Extraction (KIE), and Handwritten Mathematical Expression Recognition (HMER).

- Text Recognition: Evaluate LMM with widely-adopted OCR text recognition datasets from 8 perspectives.
- Scene Text-Centric VQA: Test LLMs on five datasets.
- Document-Oriented VQA: Assess LLMs on three datasets.
- Key Information Extraction: Conduct experiments on three datasets.
- Handwritten Mathematical Expression Recognition: Evaluate on HME100K.

In the table below, the above metrics are abbreviated for “Text Reco”, “Scene VQA”, “Doc VQA”, “KIE”, “HMER” respectively and the total sum is “Final Score”.

### B.4 GQA

We use 398 image from GQA (Hudson & Manning, 2019), a large-scale dataset for real-world visual reasoning and compositional question answering. We associate each question with the structural

Table 11: Evaluation results of Qwen-Chat-7B on the OCRBench metric.

Codec	bpp	Final Score	Text Reco	Scene VQA	Doc VQA	KIE	HMER
JPEG	0.62	311.00	68.00	119.00	70.00	54.00	0.00
	0.59	280.00	57.00	108.00	62.00	53.00	0.00
	0.54	202.00	39.00	85.00	45.00	33.00	0.00
	0.53	173.00	31.00	78.00	37.00	27.00	0.00
ELIC	0.28	467.00	167.00	145.00	85.00	70.00	0.00
	0.21	453.00	163.00	140.00	84.00	66.00	0.00
	0.16	416.00	154.00	125.00	80.00	57.00	0.00
	0.12	336.00	138.00	106.00	49.00	43.00	0.00
MSILLM	0.30	435.00	162.00	133.00	81.00	59.00	0.00
	0.21	366.00	145.00	115.00	66.00	40.00	0.00
	0.15	289.00	128.00	94.00	37.00	30.00	0.00
	0.08	101.00	49.00	34.00	18.00	0.00	0.00
RDEIC	0.11	327.00	151.00	112.00	40.00	24.00	0.00
	0.08	310.00	138.00	104.00	43.00	25.00	0.00
	0.06	284.00	129.00	100.00	34.00	21.00	0.00
	0.03	166.00	80.00	61.00	18.00	7.00	0.00

type derived from the final operation in the question’s functional program, as shown below, with the “Overall” stands for the weighted sum.

- choose: Questions that present two alternatives to choose from, e.g. “Is it red or blue ?”
- compare: Comparison questions between two or more objects.
- logical: Involve logical inference.
- query: All open questions.
- verify: Yes/No questions.

Table 12: Evaluation results of Qwen-Chat-7B on the GQA metric.

Codec	bpp	Overall	choose	compare	logical	query	verify
JPEG	0.27	48.18	70.68	55.18	63.12	31.21	74.38
	0.25	47.42	70.68	53.14	61.62	30.46	74.11
	0.20	43.20	64.92	52.63	58.74	26.48	67.94
	0.19	41.93	63.95	53.99	57.24	24.89	66.96
ELIC	0.25	54.06	75.82	57.22	69.22	37.68	79.71
	0.16	53.12	75.29	55.35	68.94	36.65	78.51
	0.10	52.67	73.16	55.52	69.72	36.11	78.06
	0.06	52.31	74.22	55.86	65.56	36.40	77.89
MSILLM	0.18	53.91	76.26	55.69	67.05	37.97	79.88
	0.09	53.32	75.38	55.69	66.72	37.49	78.73
	0.05	52.31	74.22	55.86	65.56	36.40	77.89
	0.01	43.71	66.52	52.97	61.90	26.42	67.54
RDEIC	0.12	53.83	75.91	56.54	66.06	37.90	80.42
	0.09	53.69	76.53	56.88	65.45	37.91	79.66
	0.07	53.54	76.53	55.86	65.95	37.74	79.22
	0.03	51.69	74.49	53.99	66.39	35.24	77.58

## B.5 MME (COMPREHENSIVE MULTIMODAL LLM (MLLM) EVALUATION)

MME (Chaoyou et al., 2023) aims to offer a comprehensive evaluation suite that jointly measures perception and cognition for MLLMs across 14 subtasks. We only test the perception part for 1187 compressed images, which on top of OCR includes the recognition of coarse-grained and fine-grained objects. The “Overall” stands for the sum of all perception metrics.

- OCR: Optical Character Recognition (OCR) is a foundational capability of MLLMs, serving for subsequent text-based tasks such as text translation and text understanding.
- Coarse-Grained Recognition: The contents of coarse- grained recognition include the existence of common objects, and their count, color, and position. In each perception subtask, we prepare 30 images with 60 instruction-answer pairs.
- Fine-Grained Recognition: The fine-grained recognition is more about testing the knowledge resources of MLLMs. The subtasks consist of recognizing movie posters, celebrities, scenes, landmarks, and artworks, containing 147, 170, 200, 200, and 200 images respectively.

Table 13: Evaluation results of Qwen-Chat-7B on the MME metric.

Codec	bpp	Overall	OCR	artwork	celebrity	color	count	existence	landmark	position	posters	scene
JPEG	0.30	1236.7	80.0	95.0	76.8	146.7	108.3	180.0	108.0	128.3	150.3	163.2
	0.27	1208.5	87.5	87.8	73.5	141.7	103.3	180.0	97.0	120.0	153.7	164.0
	0.23	1017.5	72.5	74.0	53.5	128.3	93.3	151.7	74.2	81.7	135.7	152.5
	0.22	971.8	62.5	75.5	52.4	138.3	76.7	140.0	66.5	86.7	127.6	145.8
ELIC	0.21	1367.6	65.0	103.0	109.4	175.0	138.3	185.0	141.0	128.3	156.8	165.8
	0.14	1321.7	80.0	96.2	100.0	163.3	123.3	180.0	136.2	121.7	155.1	165.8
	0.09	1288.4	72.5	95.0	85.6	170.0	126.7	175.0	123.5	121.7	151.0	167.5
	0.06	1226.8	72.5	90.2	71.2	161.7	106.7	175.0	114.5	123.3	149.0	162.8
MSILLM	0.18	1382.6	72.5	112.0	115.9	180.0	125.0	185.0	147.5	116.7	163.3	164.8
	0.10	1394.9	87.5	115.5	113.5	185.0	123.3	185.0	139.2	126.7	156.1	163.0
	0.06	1325.6	65.0	110.2	93.2	175.0	106.7	185.0	136.0	135.0	153.4	166.0
	0.02	1066.4	80.0	95.0	40.6	148.3	105.0	140.0	98.0	110.0	102.7	146.8
RDEIC	0.12	1408.4	72.5	119.2	120.9	180.0	140.0	190.0	146.5	125.0	151.0	163.2
	0.09	1428.6	95.0	122.2	118.8	175.0	140.0	190.0	147.8	130.0	147.3	162.5
	0.07	1395.9	87.5	119.0	107.4	170.0	135.0	195.0	146.2	125.0	147.3	163.5
	0.03	1311.4	95.0	111.2	84.1	165.0	110.0	185.0	141.8	115.0	139.8	164.5

## B.6 MMBENCH

MMBench (Liu et al., 2024a) is a systematically designed objective multi-modality benchmark for a robust and holistic evaluation of VLMs with 4329 images covering 20 ability dimensions. “Overall” is the weighted average of the above six metrics.

- AR: Attribute Reasoning.
- CP: Coarse Perception
- Fine-grained Perception: FP-C, cross-instance; FP-S, single-instance.
- LR: Logical Reasoning.
- RR: Relation Reasoning.

## B.7 SEEDBENCH

SEED-Bench (Li et al., 2023a) consists of 19K multiple choice questions with accurate human annotations, which spans 12 evaluation dimensions including the comprehension of both the image and video modality. We evaluate VLMs on 14232 images across 9 dimensions, involving only spatial understanding. “Overall” is the weighted average of the above metrics.

Table 14: Evaluation results of Qwen-Chat-7B on the MMBench metric.

Codec	bpp	Overall	AR	CP	FP-C	FP-S	LR	RR
JPEG	0.29	36.68	35.68	48.99	30.77	44.71	12.71	18.26
	0.27	35.91	36.18	45.61	30.77	45.39	13.56	15.65
	0.24	30.67	31.16	41.89	25.87	35.84	14.41	10.43
	0.23	27.66	33.17	35.81	20.98	30.38	16.10	10.43
ELIC	0.20	43.56	38.19	60.47	37.06	51.19	16.95	25.22
	0.13	41.75	36.18	60.14	37.06	48.46	14.41	20.87
	0.09	41.49	37.19	58.11	34.97	49.83	16.10	19.13
	0.06	37.63	35.18	51.69	31.47	44.03	12.71	22.61
MSILLM	0.17	42.53	38.69	61.15	30.77	49.83	14.41	26.09
	0.10	43.64	39.20	60.47	35.66	51.19	16.10	26.96
	0.06	42.70	41.21	60.14	37.06	49.49	10.17	23.48
	0.02	26.80	25.63	40.20	23.78	29.69	11.02	6.96
RDEIC	0.11	42.96	37.69	59.80	37.06	50.51	15.25	25.22
	0.08	43.56	35.68	60.14	37.76	52.22	15.25	28.70
	0.06	43.21	36.68	59.46	37.06	52.22	15.25	26.09
	0.02	40.55	35.18	59.12	32.17	46.76	12.71	25.22

- Instance Attributes: This dimension is related to the attributes of an instance, such as color, shape or material. It assesses a model’s understanding of an object’s visual appearance.
- Instance Identity: This dimension involves the identification of a certain instance in the image, including the existence or category of a certain object in the image. It evaluates a model’s object recognition capability.
- Instance Interaction: This dimension requires the model to recognize the state relation or interaction relations between two humans or objects.
- Instance Location: This dimension concerns the absolute position of one specified instance. It requires a model to correctly localize the object referred to in the question.
- Instances Counting: This dimension requires the model to count the number of a specific object in the image. This requires the model to understand all objects, and successfully count the referred object’s instances.
- Scene Understanding: This dimension focuses on the global information in the image. Questions can be answered through a holistic understanding of the image.
- Spatial Relation: This dimension asks a model to ground the two mentioned objects, and recognize their relative spatial relation within the image.
- Text Understanding: For this dimension, the model should answer questions about the textual elements in the image.
- Visual Reasoning: This dimension evaluates if a model is able to reason based on the visual information. This requires the model to fully understand the image and utilize its common sense knowledge to correctly answer the questions.

In the table below, the above metrics are abbreviated for “Attr.”, “Ident.”, “Interact.”, “Loc.”, “Count”, “Scene”, “Spatial”, “Text”, “Reason.” respectively.

Table 15: Evaluation results of Qwen-Chat-7B on the SEEDBench metric.

Codec	bpp	Overall	Attr.	Ident.	Interact.	Loc.	Count	Scene	Spatial	Text	Reason.
JPEG	0.28	50.71	51.09	56.47	63.92	47.03	35.39	61.94	41.86	20.24	51.96
	0.26	49.47	50.16	53.96	57.73	46.11	35.31	60.29	39.88	16.67	51.06
	0.21	46.11	46.72	48.17	52.58	43.35	34.16	56.68	35.31	22.62	47.13
	0.20	44.23	45.30	45.82	46.39	39.47	32.16	54.08	36.99	22.62	48.94
ELIC	0.21	56.74	57.90	63.35	55.67	54.29	43.11	65.83	42.31	29.76	60.73
	0.14	56.42	58.57	62.42	60.82	52.35	42.01	65.67	41.70	25.00	58.91
	0.09	55.09	56.72	61.28	58.76	51.23	40.25	64.88	42.62	28.57	56.19
	0.06	55.51	57.65	60.13	57.73	51.74	41.07	65.55	41.55	30.95	55.29
MSILLM	0.17	57.35	59.09	63.41	57.73	53.58	43.69	66.34	43.07	26.19	61.93
	0.10	56.51	58.06	61.66	59.79	53.27	42.30	66.37	43.53	26.19	59.21
	0.06	55.51	57.65	60.13	57.73	51.74	41.07	65.55	41.55	30.95	55.29
	0.02	43.25	46.29	44.40	51.55	39.98	31.30	51.49	31.66	22.62	39.27
RDEIC	0.12	57.95	59.71	64.12	58.76	54.70	44.54	66.50	44.44	25.00	61.33
	0.09	57.51	59.17	63.68	56.70	54.09	44.14	66.18	44.44	23.81	61.03
	0.07	57.37	58.34	63.52	61.86	54.91	44.42	66.50	44.29	22.62	59.21
	0.03	54.79	56.74	60.19	59.79	51.43	40.95	63.77	41.86	26.19	55.59

## C MORE BENCHMARKING RESULTS

### C.1 ADDITIONAL RATE-METRIC CURVES RESULTS

In this work, we primarily evaluate open-source VLMs because the cost of querying commercial API-based models is prohibitively high, as stated in the conclusion section of the original paper. Moreover, closed-source models cannot be used for our adaptor-based enhancement experiments, making it impossible to verify the effectiveness of the proposed method on these models. However, we conducted an evaluation on OCRBench using GPT-4o to validate the effectiveness for closed-source VLMs. The rate-metric curve is shown in Figure 11 and all outcomes are fully consistent with the findings presented in this paper.

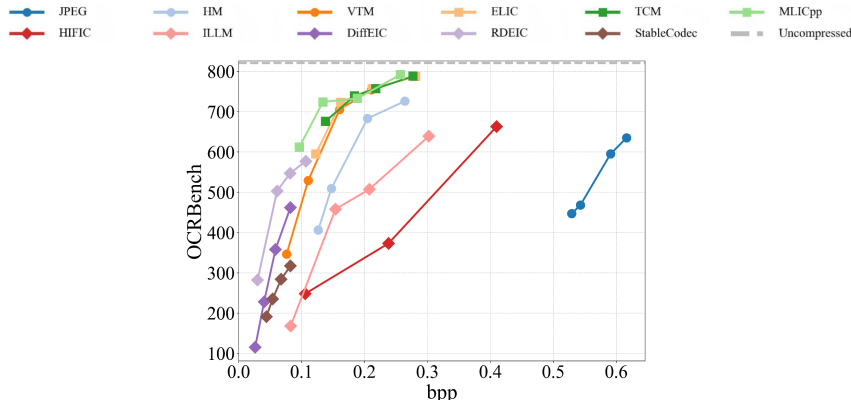


Figure 11: Rate-OCRBench curve for all types of codecs using Chatgpt-4o.

We further incorporated the COCO-Caption task using the Qwen-Chat model. By including this image captioning task, we enhance the breadth and completeness of our evaluation. Representative experimental results are presented below. We report the bpp, ROUGE-L, and CIDEr scores for three representative methods, and use CIDEr to compute the BD-Metric for all compression approaches. The outcomes remain fully consistent with the findings reported in our paper. From the curve, we observe that generative codecs achieve the best overall performance, further confirming their advantage in semantic reconstruction under low-bitrate conditions.

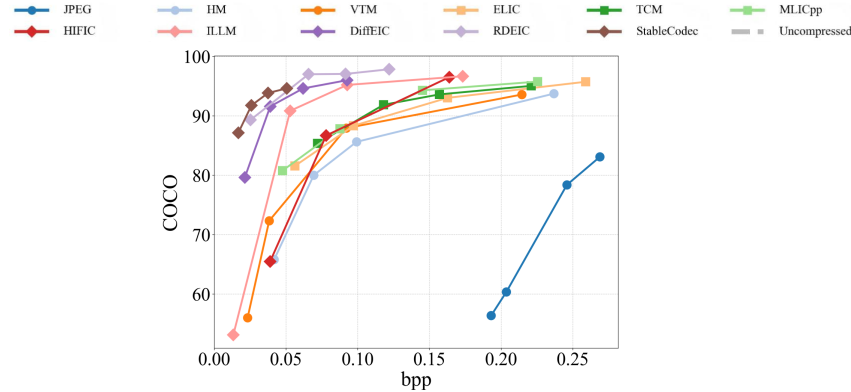


Figure 12: Rate-metric curve based on COCO-Caption task for all types of codecs using Qwen-Chat model.

Furthermore, we present additional evaluation results in the form of Rate–Metric curves. We report results for other VLMs, organized into three series of figures. Each figure includes Rate–Metric curves across all considered codecs and benchmark datasets as well as the baseline performance on uncompressed images.

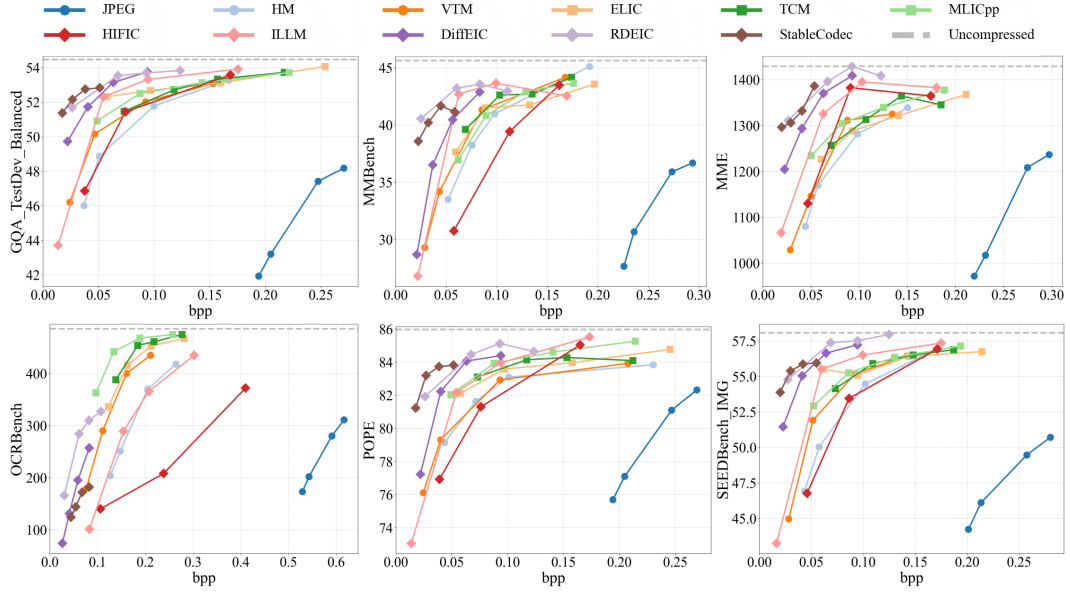


Figure 13: Rate-Metric curves for all types of codecs on GQA, MMB, MME, OCRBench, POPE, and SEEDBench using Qwen-Chat-7B.

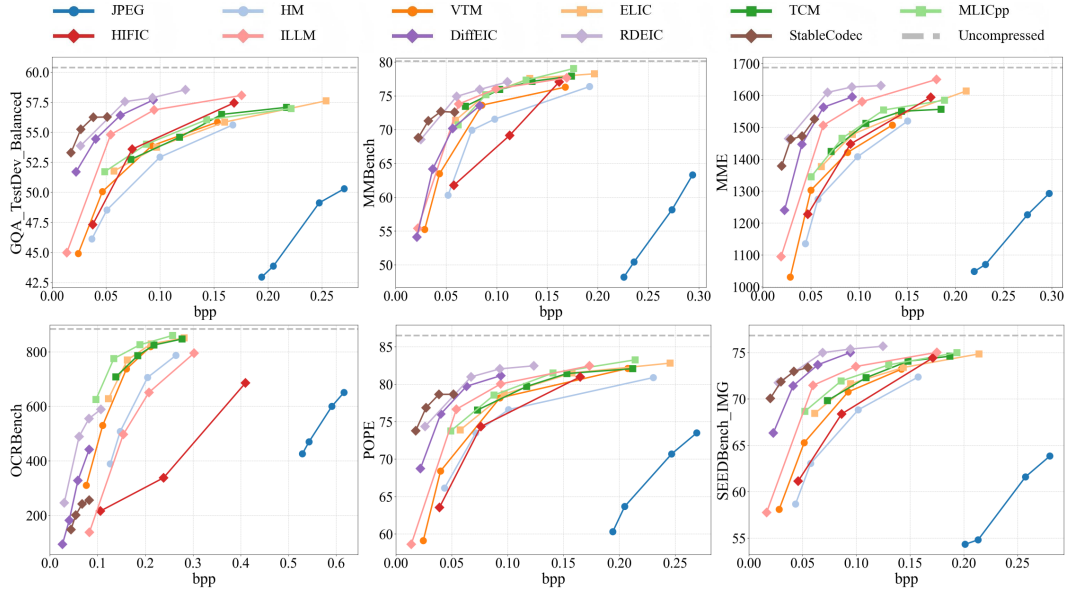


Figure 14: Rate-Metric curves for all types of codecs on GQA, MMB, MME, OCRBench, POPE, and SEEDBench using Qwen2.5-VL-7B.

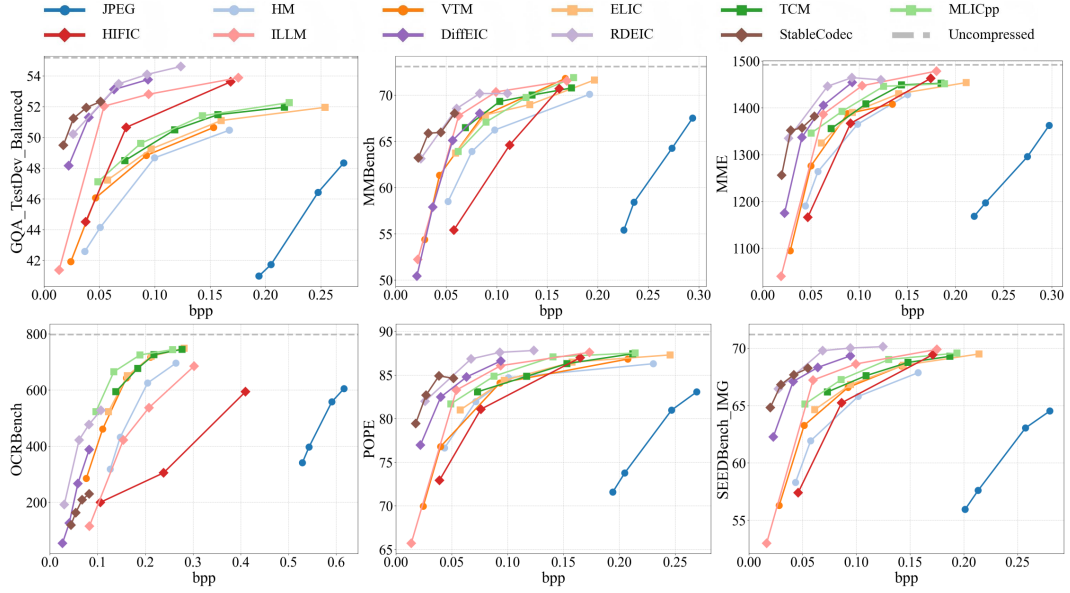


Figure 15: Rate-Metric curves for all types of codecs on GQA, MMB, MME, OCRBench, POPE, and SEEDBench using InternVL3-1B.

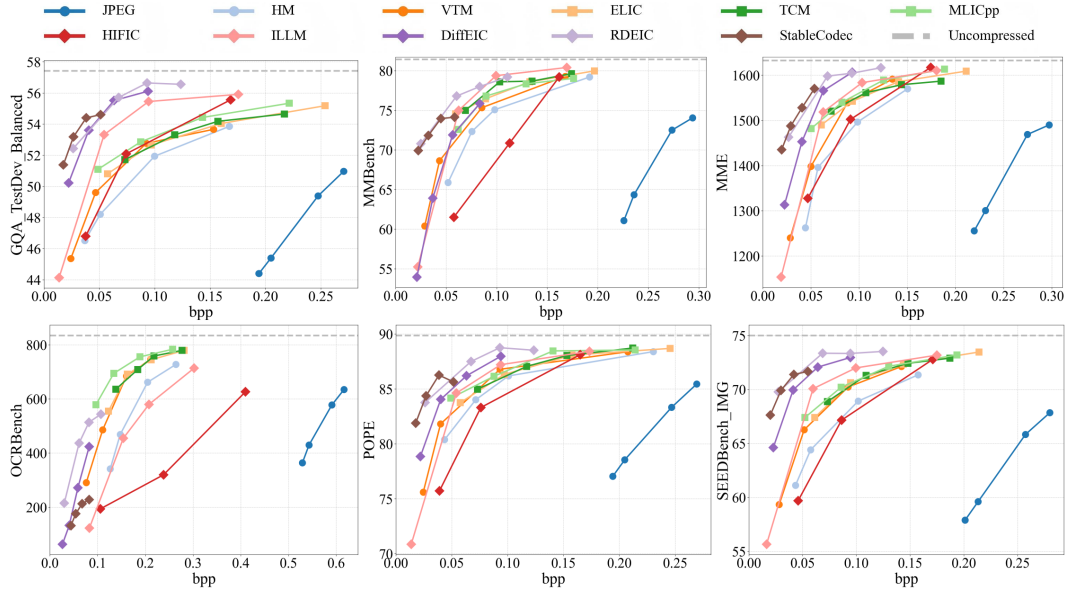


Figure 16: Rate-Metric curves for all types of codecs on GQA, MMB, MME, OCRBench, POPE, and SEEDBench using InternVL3-2B.

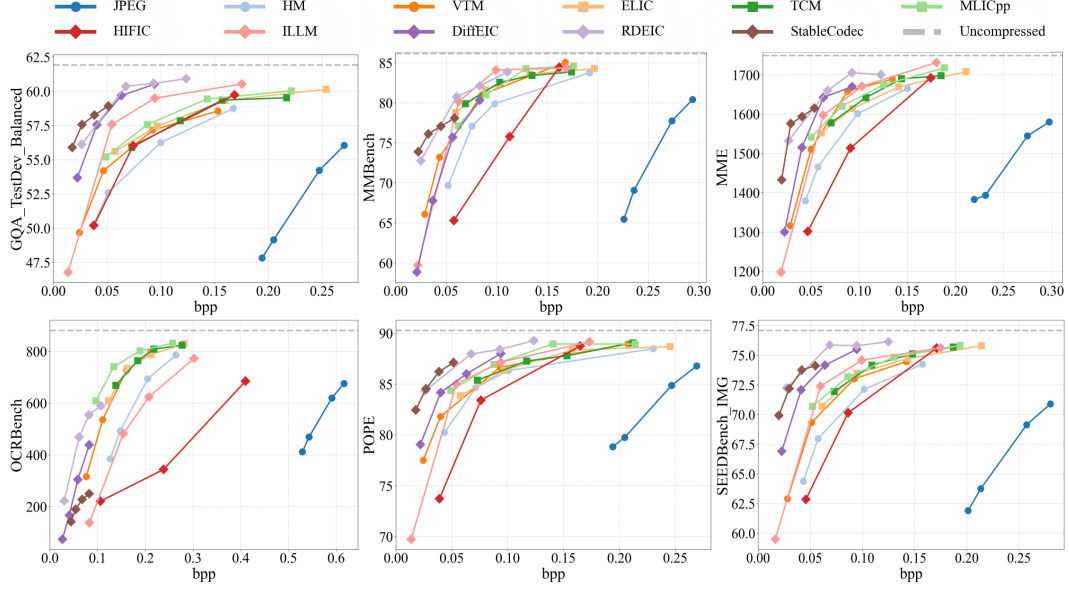


Figure 17: Rate-Metric curves for all types of codecs on GQA, MMB, MME, OCRBench, POPE, and SEEDBench using InternVL3-8B.

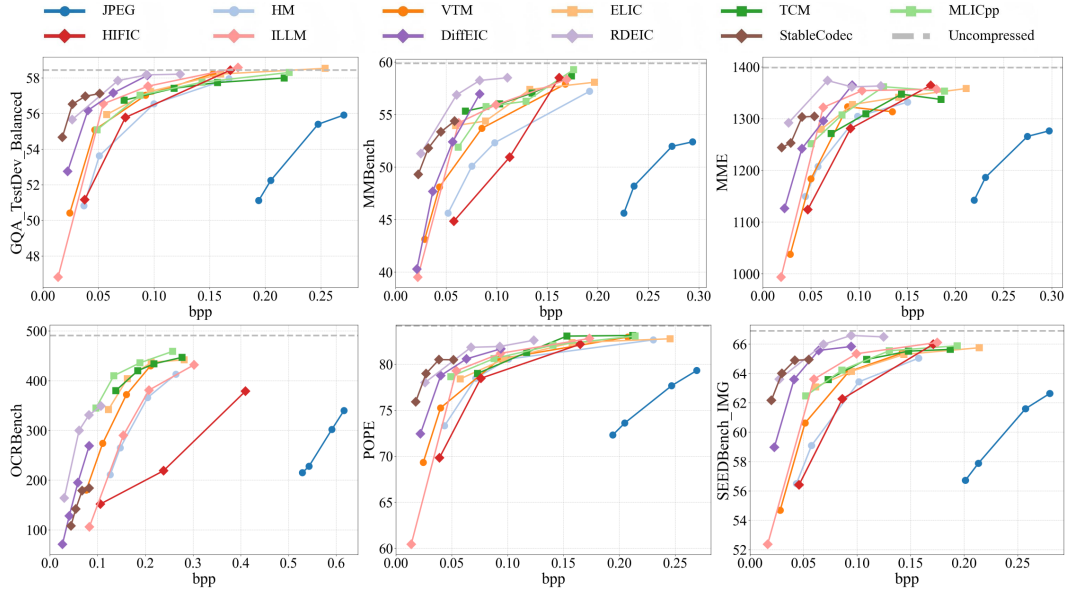


Figure 18: Rate-Metric curves for all types of codecs on GQA, MMB, MME, OCRBench, POPE, and SEEDBench using Janus-Pro-1B.

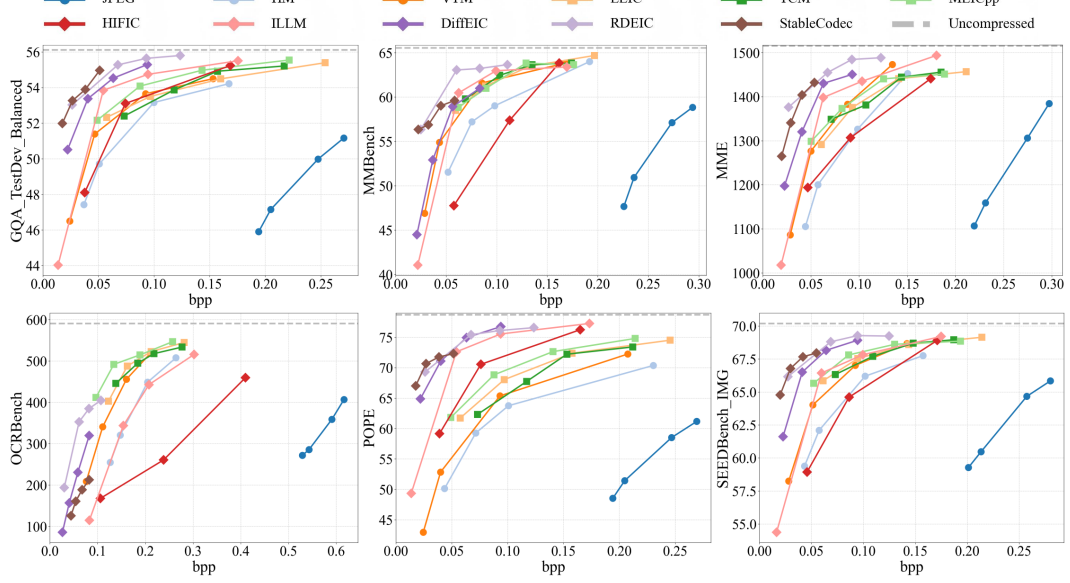


Figure 19: Rate-Metric curves for all types of codecs on GQA, MMB, MME, OCRBench, POPE, and SEEDBench using Janus-Pro-7B.

## C.2 ADDITIONAL VLMs COMPRESSION RESULTS

Figure 20 presents radar charts comparing the performance of various VLMs under three different compression codecs: JPEG, ELIC, and ILLM. Each chart visualizes model performance across six benchmarks: POPE, GQA, SEEDBench, MMB, MME, and OCRBench. Under comparable parameter scales, InternVL3 consistently outperforms Qwen2.5, which in turn surpasses Janus-Pro across all distortion conditions. This ranking is consistent with the uncompressed baseline results reported in Figure 10, reinforcing the observation that stronger models exhibit greater robustness to compression artifacts.

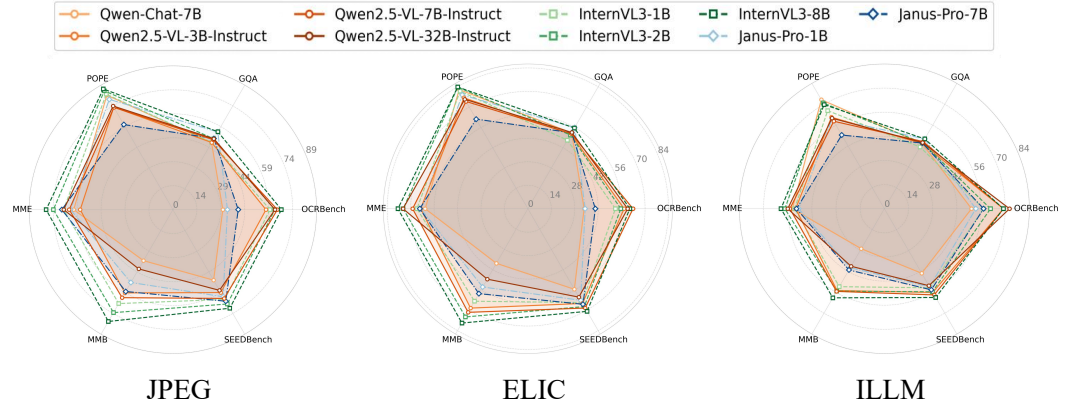


Figure 20: Visualization of various VLM models across all metrics under three different compression distortion conditions.

## C.3 ADDITIONAL BD-METRICS RESULTS

We report additional evaluation results for VLMs, which also serve as the data source for Figure 3.

Table 16: Comparison of BD-Metrics for different VLMs across various tasks. The value measures the average decrease in metrics relative to the uncompressed condition under the same compression bitrate for different codecs. Red fonts indicate the best-performing models, while blue fonts denote the second-best.

VLM	Metric	JPEG	HM	VTM	ELIC	TCM	MLIC	HiFiC	MSILLM	D.EIC	RDEIC	S.Codec
Qwen VL2.5 -3B	OCRB	-339.1	-242.4	-251.1	-98.9	<b>-86.2</b>	<b>-87.0</b>	-485.0	-308.0	-576.0	-387.6	-624.8
	GQA	-14.25	-7.63	-7.01	-4.05	-3.78	-4.07	-5.89	-3.99	<b>-3.64</b>	<b>-1.97</b>	-3.88
	POPE	-17.75	-6.16	-6.59	<b>-4.61</b>	<b>-4.68</b>	-4.81	-10.95	-7.80	-7.34	-5.44	-8.13
	MME	-506.9	-342.2	-309.6	-153.7	-142.1	-139.2	<b>-126.2</b>	-182.4	-190.0	<b>-78.0</b>	-183.6
	MMB	-27.95	-9.01	-8.03	-4.82	<b>-4.65</b>	<b>-4.66</b>	-13.23	-6.62	-12.70	-5.61	-8.20
	SEEDB	-19.08	-8.38	-7.83	-3.90	<b>-3.69</b>	-3.85	-7.55	-5.10	-3.96	<b>-1.85</b>	-3.86
Intern VL3 -2B	OCRB	-314.6	-228.0	-242.4	-116.1	<b>-104.2</b>	<b>-106.5</b>	-483.5	-325.4	-597.8	-395.4	-639.3
	GQA	-9.50	-5.97	-5.72	-3.72	-3.73	-3.51	-4.86	-3.52	<b>-2.87</b>	<b>-1.89</b>	-3.70
	POPE	-8.28	-3.40	-3.61	<b>-2.45</b>	<b>-2.38</b>	-2.46	-5.98	-4.61	-4.67	-2.50	-4.76
	MME	-230.8	-151.6	-143.9	<b>-60.6</b>	-65.8	-60.9	-137.8	-105.3	-117.4	<b>-51.7</b>	-121.3
	MMB	-12.07	-5.74	-6.50	<b>-3.43</b>	<b>-3.09</b>	-3.94	-11.86	-5.62	-12.79	-4.92	-8.60
	SEEDB	-11.62	-6.87	-6.30	<b>-3.28</b>	-3.35	-3.60	-7.21	-4.95	-4.12	<b>-2.19</b>	-4.48
Intern VL3 -1B	OCRB	-303.7	-226.7	-236.6	-110.6	<b>-101.5</b>	<b>-104.3</b>	-458.3	-321.7	-571.9	-381.1	-609.2
	GQA	-10.51	-7.25	-7.08	-4.64	-4.29	-4.44	-4.28	-3.40	<b>-2.96</b>	<b>-1.91</b>	-3.66
	POPE	-11.38	-5.15	-6.14	-3.96	-3.98	<b>-3.59</b>	-7.69	-5.88	-5.95	<b>-3.25</b>	-6.09
	MME	-231.9	-142.5	-153.1	-75.4	<b>-68.4</b>	-69.0	-137.5	-96.1	-119.9	<b>-56.7</b>	-143.6
	MMB	-10.94	-6.20	-5.64	-4.33	<b>-3.65</b>	<b>-4.30</b>	-9.88	-5.08	-10.94	-4.75	-7.16
	SEEDB	-10.30	-6.09	-5.92	-3.23	-3.09	<b>-2.91</b>	-5.90	-4.27	-3.64	<b>-1.83</b>	-4.02
Janus -pro -1B	OCRB	-217.5	-151.3	-160.3	-71.8	<b>-65.9</b>	<b>-66.2</b>	-251.6	-163.2	-314.7	-196.2	-330.3
	GQA	-4.24	-2.33	-2.04	<b>-0.57</b>	-0.88	-0.99	-2.17	-1.92	-1.82	<b>-0.81</b>	-1.82
	POPE	-8.00	-3.45	-3.90	<b>-2.53</b>	<b>-2.22</b>	-2.61	-5.67	-5.05	-4.69	-2.82	-4.66
	MME	-164.6	-116.7	-138.3	<b>-62.7</b>	-75.6	-63.8	-128.4	-90.6	-123.1	<b>-42.7</b>	-119.2
	MMB	-9.38	-6.49	-6.15	-3.47	<b>-3.17</b>	-3.69	-9.68	-5.60	-9.15	<b>-3.29</b>	-7.30
	SEEDB	-6.77	-4.37	-4.20	-2.00	<b>-1.80</b>	-1.94	-4.33	-3.21	-2.53	<b>-1.08</b>	-2.60
GPT-4o	OCRB	-276.8	-208.8	-199.7	<b>-83.2</b>	<b>-74.4</b>	-91.6	-422.0	-347.6	-506.1	-329.0	-556.6

#### C.4 ADDITIONAL SCALING LAW RESULTS

In this section, we provide additional metrics for the InternVL3 model series, as shown in Figure 21. These results are consistent with the main findings: the scaling laws don't apply to compressed images.

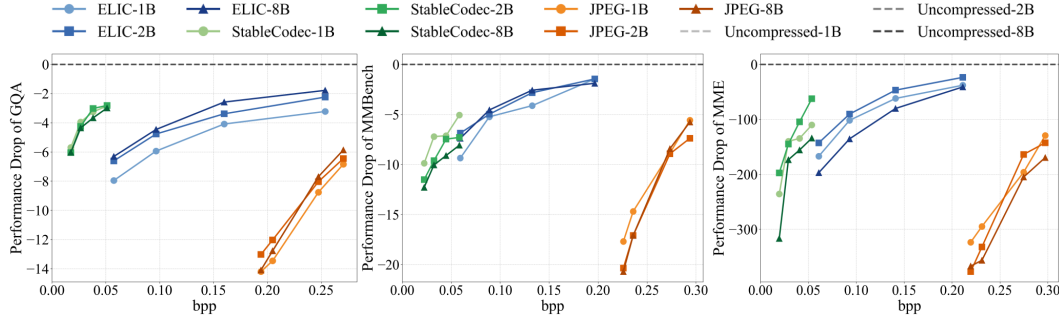


Figure 21: Rate-Metric drop curves to validate the scaling law based on InternVL3 series models.

Additionally, we report results for the Qwen2.5-VL model series with 3B, 7B, and 32B parameters across different codecs, as shown in Figure 22. Interestingly, the 32B variant underperforms the 7B model on uncompressed images. Due to the lack of publicly available technical details for Qwen2.5-VL-32B, we are unable to verify this discrepancy. Nevertheless, the overall trend is clear: larger model size does not necessarily correspond to lower performance drop under compression.

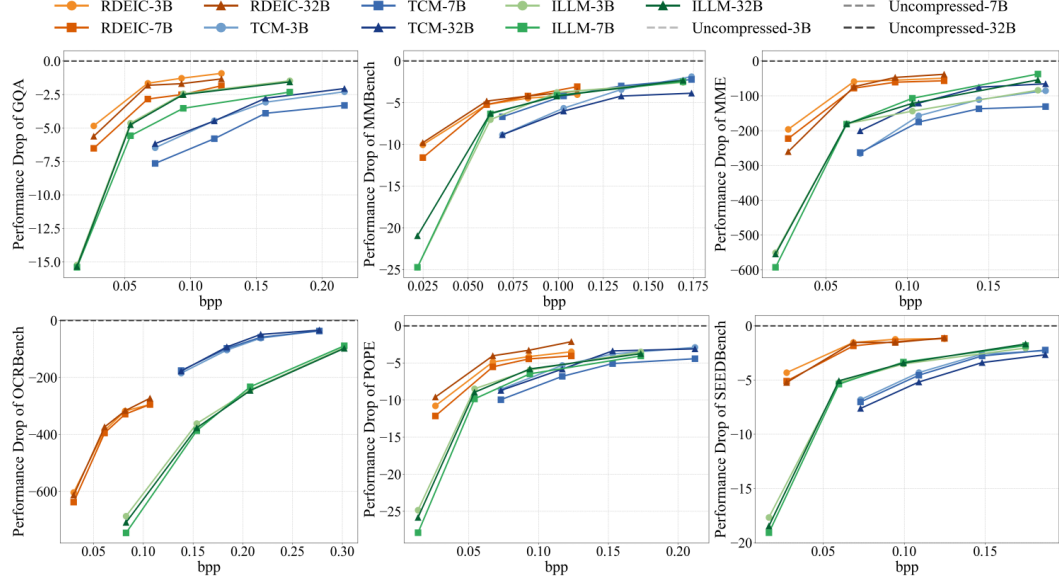


Figure 22: Rate-Metric drop curves to validate the scaling law based on Qwen-VL2.5 series models.

## D MORE ENHANCEMENT RESULTS

We have supplemented our experiments with a comprehensive set of additional benchmarks, including GQA, MMBench, OCRBench and MME. As shown in Figure 23 and Table 17, the additional results consistently confirm the effectiveness of our adaptor across all evaluated settings, demonstrating its robustness to diverse compression distortions and validating its claim as a generalizable solution.

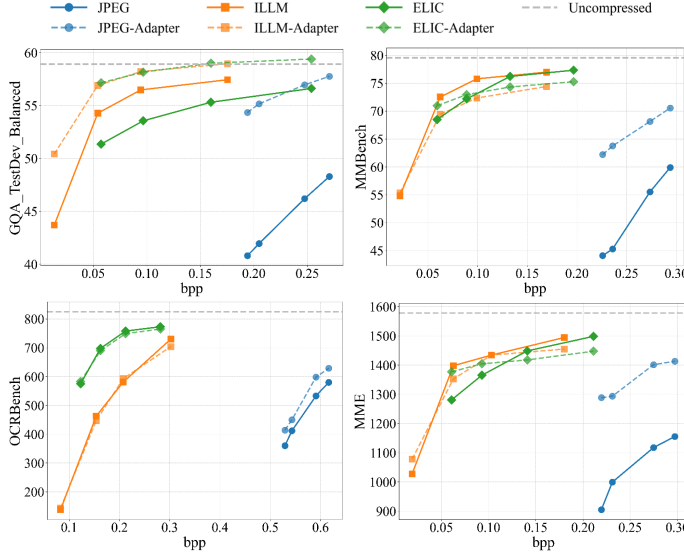


Figure 23: Rate-accuracy comparison on GQA, MMBench, OCRBench and MME using QwenVL2.5-3B model.

Table 17: The BD-Metric results are compared against the original compression outcomes using QwenVL2.5-3B.

	<b>Codec</b>	<b>JPEG</b>	<b>ELIC</b>	<b>ILLM</b>
BD-GQA	11.63	3.88	2.38	
BD-MMB	14.91	2.45	0.86	
BD-OCR	52.51	10.51	14.34	
BD-MME	285.4	75.97	19.72	